CERN/SPSLC 95-20
SPSLC/M542
20 March 1995

CERES/NA45 Report to Cogne 1995

P. Holl, H. Kraner, P. Rehak
Brookhaven National Laboratory, Upton, USA

J. Schukraft
CERN, Geneva, Switzerland

G. Agakichiev, Y. Minaev, Y. Panebrattsev, S. Razin, S. Shimanskiy, V. Yurevich
JINR, Dubna, Russia

F. Ceretto, U. Faschingbauer, Ch. Fuchs, J. P. Wurm
Max-Planck-Institut für Kernphysik, Heidelberg

E. Gatti, M. Sampietro
Politecnico di Milano, Italy

R. Baur, A. Drees, P. Glässel, B. Lenkeit, M. Messer, A. Pfeiffer, H. J. Specht, T. Ullrich, C. Voigt
Universität Heidelberg, Germany

Z. Fraenkel, C. P. de los Heros, I. Ravinovich, E. Socol, G. Tel-Zur, I. Tserruya (Spokesman)
Weizmann Institute, Rehovot, Israel

Contents

1 Introduction

CERES/NA45 is the only heavy-ion experiment dedicated to the measurement of e^+e^- pairs at ultra-relativistic energies. For that purpose, we have developed a novel spectrometer (see Fig. 1) optimized for minimum response to hadronic species: two ring imaging Cherenkov counters (RICH-1,2) with high threshold are combined with an azimuthally symmetric magnetic field, accepting electron pairs from the low-mass region to beyond 1 GeV/c^2, limited at the upper end only by the accessible statistics (see refs. [1, 2, 3, 4]). The spectrometer covers the mid-rapidity region with 2π azimuthal symmetry and accepts a very broad range of $p_\perp$. Since 1994 a stand-alone external tracking into RICH-1 has been incorporated by replacing the single silicon-drift chamber (SIDC) [5] by a closely spaced doublet of two such detectors of improved specifications. The powerful recognition of close electron pairs from conversions and Dalitz decays by this doublet together with the RICH-detectors is essential to reduce the combinatorial pair background. As a reward, it enables us also to measure photons by the conversion method, in the $p_\perp$-range of 0.4 to 2.0 GeV/c, with much improved systematical errors.

Dileptons and direct photons supply a unique probe for studying the early collision dynamics. The argument dates back more than sixteen years when it was first proposed by Shuryak [6], and it is simple: being electromagnetic radiation, their mean free path is large compared to the size of the interaction system and, once produced, they can leave freely without further interactions. The physics potential attached to those penetrating probes derives from the fact that their luminosity (or production rate), as of any electromagnetic radiation, is a strongly increasing function of the temperature. They are therefore most abundantly produced at the early stages when temperature and energy density have their highest values. It should be stressed that most of the present knowledge on the collision dynamics originates from hadronic observables and is therefore restricted to the late stages of the freeze-out.

The search for thermal radiation, either from the conjectured quark-gluon plasma via the $q\bar{q}$ annihilation process, or from the dense hadronic matter in a mixed phase via $\pi^+\pi^-$ annihilation into e^+e^-, is the main subject of interest. Readily accessible to CERES is the thermal pair radiation in the low-mass region, and we put emphasis below on the new physics to be learned from it. Thermal pair production out of the deconfined phase might be observable only in the intermediate mass range [7, 8]. As will be detailed in Section 3 of this document, a sufficient data sample also above $m \simeq 1$ GeV/c^2 is not beyond the

reach of CERES in the future.

To elucidate the unique pursuit of CERES further, we consider a potential signal of the onset of the restoration of chiral symmetry which is predicted to occur along with the deconfinement transition. The excitation and properties of ρ mesons might be strongly modified by chiral restoration. Due to the short life time of τ= 1.3 fm/c the decay $\rho \rightarrow e^+e^-$ will occur within the dense matter, and the mass spectrum of electron pairs will convey such transition. In the hadronic observables, i.e. $\rho \rightarrow \pi\pi$, such information is lost, due to the rescattering of the hadrons in the dense matter. The other vector mesons, ω and ϕ, which CERES measures via their e^+e^- decay channels, are an equally important part of the physics program. The measurement of direct photons also addresses the question of the thermal radiation and adds complementarity to the low-mass electron pairs.

Since the submission of our Pb proposal to the SPSLC a year ago [2], the tedious analysis of the 200 GeV/nucleon S-Au data taken in 1992 converged to a surprising result: the yield of low-mass electron pairs per charged particle displays a strong enhancement over the hadronic contribution from light-meson decays, i.e. it is not described by a mere superposition of p-p collisions. This observation indicates the onset of new physics already at energy densities and space-time volumes of the fireball attainable with light ions (sulphur) – a promise that could be scrutinized by a full-scale CERES run at the Pb beam. Such endeavor is also peremptory, given the circumstantial advantages of an instrument greatly advanced as compared to the situation prevailing in 1992, with the prospect of a much better data sample, both in size and quality, and most important, in its physics potential.

Some of our previous results and the perspectives with Pb beams are presented in Section 2; they are also discussed in a broader context comparing them to other experiments which measure muon pairs.

A short test run with a Pb beam took place last November with a large fraction of the scheme to upgrade the CERES spectrometer [2] implemented in the setup. The results of this run demonstrate that the upgraded spectrometer is able to cope with the highest multiplicities attainable in Pb-Pb collisions. Based on that, we give in Section 3 a brief description of the expected performance of the upgraded spectrometer including the sample sizes.

In Section 4 we glance into the more distant future. We presently study the possibilities (i) to measure electron pairs at a lower bombarding energy where conditions of

highest baryon density may be achieved, (ii) to measure charm production through semi-leptonic decays, and (iii) to possibly add a high-precision electromagnetic calorimeter to the present setup. Section 5 contains a short summary.

2 Physics Results and Perspectives

CERES has taken data in the years 1992-1993 [3]. We will focus here on the 1992 S-Au data for electron pairs and photons from central interactions, and on the 1993 p-Be and p-Au data for reference. The results of the S-Pt run aimed at electron-pair production in distant collisions ('QED pairs') are given in ref. [9].

To set the frame of reference, CERES collected a large sample of electron pairs from 450 GeV p-Be and p-Au collisions in 1993, taking advantage of a sizable enrichment factor by the second-level trigger. The prime goal of this systematic approach was to establish whether there is any deviation of the e^+e^- spectrum with respect to the contributions from the known hadron decay sources. The collection of inclusive pairs was supplemented by an exclusive measurement of the $e^+e^-\gamma$ and $e^+e^-\pi^\circ$ decays of the light pseudoscalar and vector mesons, respectively, in combination with the electromagnetic calorimeter of the TAPS collaboration.

The analysis of the invariant mass spectra measured in p-Be and p-Au at 450 GeV shows good agreement with the predictions based on the the known hadron decay sources (see Fig. 2). This confirms the results recently reported by HELIOS/1 on measurements of electron and muon pairs in p-Be collisions at 450 GeV [10]. The common conclusion is that there is no need to invoke any additional source. The present level of sensitivity to any direct contribution is limited by the systematical errors which are about 40%. We expect to significantly improve this limit using the $e^+e^-\gamma$ coincidence data.

The situation is very different in the S-Au system. The mass spectrum has a different shape and the observed yield is much larger than the one predicted from hadron decays. The excess starts at masses $\gtrsim 200$ MeV/c^2 and persists up to the highest masses covered in the experiment above the ρ meson. The enhancement factor, defined as the ratio of the integral of the data over the integral of the predicted sources, is found to be $5.0\pm0.7(\text{stat.})\pm2.0(\text{syst.})$ in the mass region $0.2 < m < 1.5$ GeV/c^2. Detailed accounts of these measurements can be found in refs. [11] (which is attached to this report) and [12].

This enhancement is an outstanding result of CERES. Recent results of HELIOS/3 also reveal an enhanced production of low-mass $\mu^+\mu^-$ pairs in S-W relative to p-W

collisions [13]. However, the enhancement factor – which we have derived from their data as the integral of the S-W data over the integral of the p-W data in the comparable mass range – is much smaller, ~1.6. This difference can be accounted for by a non-linear (quadratic?) dependence of the underlying production mechanism. Indeed, the average charged-particle densities accessible by the two experiments, and hence the energy densities, differ by at least a factor of two (due to the more central rapidity coverage of the CERES experiment).

HELIOS/3 also sees an enhancement over the expected yield from Drell-Yan and open charm decays in the intermediate-mass region. In the mass interval from 1.5 to 2.5 GeV/c^2 they report an enhancement of 2. The NA38 experiment, mainly focussed on the study of the J/ψ, has reported a similar result.

A common and very interesting message emerges therefore from the three dilepton experiments; they all observe an excess production of dileptons in S-induced interactions which covers the whole mass region from $m \simeq 200$ MeV/c^2 up to the J/ψ and a broad rapidity range (see [14] for a recent review of experimental results on electromagnetic probes). These results have triggered an intensive theoretical activity which is presently being pursued to assess the origin of the excess. The attention is focussed in particular on the electron data, which have been measured at mid-rapidity and are therefore more easily accessible to calculations using standard hydrodynamical models. A possible explanation comes immediately to mind from the properties of the observed dilepton excess (in electron and muon pairs): its onset at $m_{\ell\ell} \sim 2m_\pi$, the persistence of the enhancement in the ρ-mass region and the possibility of a quadratic dependence with multiplicity suggest that it is dominated by two-pion annihilation $\pi^+\pi^- \rightarrow \ell^+\ell^-$ [8, 15, 16]. This would then be the first indication of radiation emitted from the dense hadronic matter formed in relativistic heavy-ion collisions. This hypothesis is being pursued in a standard hydrodynamical scenario with and without invoking a phase transition to a QGP. Modified approaches are also being considered, like for instance a decrease of the ρ-meson mass (appearing in the pion form factor) in dense hadronic matter which has been advocated as a precursor of chiral symmetry restoration [17].

Our short term goals remain essentially as outlined in our Pb proposal [2], but they receive new stimulus by the recent results. Our Pb test run last November has clearly established that the upgraded spectrometer can cope with the highest multiplicities attainable in central Pb-Au collisions. We are therefore eagerly waiting to get new and better data to shed more light on the low-mass dilepton excess. It will be very interesting

to study the evolution of the effect under the better conditions offered by the Pb beam: the interaction volume increases to the largest value attainable in the laboratory, the multiplicity range also increases by approximately a factor of three and the energy density is somewhat larger. We also expect to get additional information (which could not be obtained from the limited statistics of our S-Au sample), in particular the multiplicity dependence and the $p_\perp$-distribution of the excess. The multiplicity dependence is a key question; CERES with its acceptance coverage close to mid-rapidity is well suited for this study.

In the near future, we expect to increase the CERES rate capability so that we will be able to study the intermediate mass range (above the ϕ and below the J/ψ resonances).

In the search for direct photons, CERES had a run on S-Au central collisions in 1992. The inclusive photon $p_\perp$-distribution and the multiplicity dependence of their yield are reproduced by the hadronic sources, within the present level of systematical errors of about 10% [18]. These results are consistent with the recent reanalysis of the WA80 data [19]. The lack of signal in the photon data is qualitatively consistent with the excess observed in the electron pairs, considering the different level of sensitivity of the two measurements with respect to their hadronic background [14]. For Pb we expect to increase the level of sensitivity to any thermal source by substantially reducing the systematic errors below the present level of $\sim$10%. For the study of electron pairs electromagnetically produced in distant Pb-Au collisions we also refer to our Pb proposal [2].

3 Performance of the Upgraded Spectrometer

In 1994 CERES had a 10 day test run with Pb ions. The prime goal was to demonstrate the feasibility of the experiment in the environment of central Pb-Pb collisions. The spectrometer has been upgraded according to the scheme described in the Pb proposal [2] (see Fig. 1) with the following priorities: (i) implementation of a new silicon drift detector system of improved design and integrated front-end electronics, (ii) an improved readout for RICH-2, and (iii) an acceleration of the data acquisition (DAQ) by one order of magnitude. The pad chamber for external tracking behind RICH-2 was postponed till 1995. Such streamlining was advocated by the necessity to fulfill that goal within the short time span of less than 8 months available with utmost certainty.

The data quality of both RICH detectors and the silicon drift chambers experienced in the test run surpassed our expectations. In Appendix A we give a detailed description of

the running conditions, and the results concerning the detector response to central Pb-Au events. Here we only give the highlights and present the sample sizes which we expect to obtain. It should be noted that the off-line analysis, optimizing the pair reconstruction efficiency under tracking conditions, together with the rejection power of close pairs of the full spectrometer, is still in progress. The results we quote here should therefore be considered as preliminary, and there is quite some room for improvements.

3.1 Summary of the Pb Test Run Results

The major part of the upgrade was implemented in time for the test run, such that the setup was very close to the final scheme proposed in ref. [2] and shown in Fig. 1. In addition, all measures directed towards reducing the background in the RICH detectors and improving their data quality were also implemented. However, a large fraction of the beam time had to be devoted to get a clean beam focussed onto our small segmented Au target. All these efforts turned out to be very beneficial for RICH-1 in particular; the unexplained hit background found in RICH-1 in our 1992 S-Au run [3] has practically disappeared. In both RICH detectors the UV photon hits show the expected linear increase with the event multiplicity, and the magnitude as well as the multiplicity dependence are well reproduced by our Monte Carlo simulations.

The silicon-drift detectors installed were highly superior to those previously used due to a better approximation of a radial drift geometry. All shortcomings in detector response and operating conditions adversely affecting the detector efficiency of the silicon drift detector in previous years have been overcome. Laser tests gave the expected resolution in the radial and azimuthal directions. The doublet of silicon chambers allows the vertex reconstruction with an almost 100% efficiency and a complete separation of the individual disks of the segmented target. The rejection of close pairs (γ conversions and π^0-Dalitz decays) has already reached the level of 80% using only the double-dE/dx information of the doublet, without invoking double-hit recognition and the additional benefit of RICH-1.

All the hardware associated with the new data acquisition system was installed prior to the run, such that data could be read out with the new scheme, but not yet at the ultimate speed. The work has progressed over the last months and, in particular, the necessary speed for the data transfer has been demonstrated. This gives us confidence that the new system will be ready for the 1995 Pb run allowing to store about 1000 events/burst on tape, an order of magnitude above the capabilities of the 1992 S run.

3.2 Expected Data Samples and Quality

In order to illustrate the future physics potential, we show in Fig. 3 the e^+e^--pair spectrum for central collisions ($dN/dy = 500$). The total yield, normalized to charged particles, includes the enhancement factor of 5 and displays the spectral shape as observed by CERES in the low-mass region for S-Au collisions. We assume that the enhancement scales with energy density and hence remains nearly unchanged in central Pb-Pb collisions. The spectral shape above the ϕ meson can be judged by the HELIOS/3 data – assuming no strong y-dependence. For that purpose the HELIOS/3 data have been normalized to our data in the low-mass region implying the same underlying physics. For reference, the figure displays the expected combinatorial background and the contribution from light meson decays ($\pi^\circ, \eta, \rho, \omega, \phi$) based on our Monte-Carlo simulations. According to the simulation the signal-to-background ratio is about 2 and the reconstruction efficiency is ~16%. The expected mass resolution is adequate to resolve the vector mesons ρ/ω from the ϕ meson if they are not masked by the direct pair production.

The e^+e^--pair sample expected in 30 days (with a 100% running efficiency) is summarized in Table 1. We consider a trigger scheme with two multiplicity thresholds, one at $dN/dy > 100$ intended to cover a large range of multiplicity densities, scaled down by a factor of 3, and a second at $dN/dy > 400$ providing a higher statistics sample of central collisions. For masses above 200 MeV/c^2 and a single track $p_\perp$-cut of 200 MeV/c, we expect 4000 to 5000 reconstructed e^+e^--pairs from hadron decays for each of the two multiplicity bins. Adding the direct source of low-mass pairs, as we measured it in S-Au collisions, gives a five times larger sample. The last entries in Table 1 subdivide the samples in different mass regions. It is evident that a high accuracy can be reached for low masses and even reasonable samples are accumulated for the ϕ-meson mass range, sufficient not only to quantify the enhancement, but also to study in detail its properties.

The sample beyond the ϕ meson is limited by the rapidly decreasing production cross section, and about a factor of 10 more statistics is needed to obtain significant data up to ~2 GeV/c^2. Several factors limit the beam intensity – the production of δ-electrons, the load on the UV detectors, and the radiation safety – to a maximum value of a few 10^6 ions/burst. Our second-level trigger has the potential to increase the data sample by a factor of 3 to 10, but the full benefit will only be achieved for unrealistic beam intensities of several 10^7. The obvious solution left is to record practically all offered first-level triggers.

We are now considering a concept to reduce the deadtime of the data acquisition

system as developed for 1995/96 by still an additional order of magnitude, down to 300 μs per event. The main idea is to employ a pipelined system, i.e. buffering the events at the level of the readout electronics before they are collected by the DAQ. As a consequence of the reduced deadtime, 4000 out of 5000 first-level triggers can be accumulated on tape for a beam rate of $5 \cdot 10^6$ ions/burst. However, in order to safely operate the spectrometer at this beam intensity, any microstructure of the beam needs to be avoided, and in addition, the sensitivity of CERES to pile-up beam particles has to be further reduced. A data acquisition system based on this scheme could become available in about 2 years.

A measurement of inclusive photon production will be performed in a dedicated run, optimized for minimum systematical errors, as outlined in our Pb proposal. We will use the converter method, with the converter located between the two SIDC's. This is an ideal location, which allows a positive and rather unambiguous identification of photon conversions, independent of the RICH detectors, by the absence of a hit in SIDC-1 and a double-dE/dx signal or two close hits in SIDC-2. In Table 2 we give the revised expected sample size. A total of 4 days will be needed for a set of two measurements using two different absorber thicknesses.

4 Perspectives for the More Distant Future

In this section we briefly present some ideas to complement and enlarge the scope of the CERES physics program beyond the years of 1995 – 1996/97.

4.1 Measurements at Lower SPS Energies

The origin of the dilepton excess observed by CERES, HELIOS-3 and NA38 is a key question which has to be addressed as a joint experimental and theoretical effort. One possible way to get additional information would be the study of dileptons at a lower incident energy. This measurement is very attractive as it will help filling the huge energy gap, between the BEVALAC or SIS on one side and the CERN SPS on the other side, where there is no information whatsoever on dilepton production in heavy-ion collisions. More specifically, as mentioned in Section 2, one possible explanation for the observed dilepton excess is based on a medium modification of the ρ in dense hadronic matter, connected to chiral symmetry restoration. If so, it would be of extreme interest to run, at least once, at a beam energy corresponding to the maximum baryon density in the full-stopping regime, i.e. at an energy somewhere between 20 and 60 GeV/nucleon. Since

other ion experiments will surely also be interested to run once under such conditions, we propose to operate the SPS Pb beam either in 1997 or 1998 for an extended period at the lowest SPS energy which is technically feasible (about 30 GeV/nucleon at the time of writing).

4.2 Open Charm Production

The production of charm quark-antiquark pairs ($c\bar{c}$) is expected to be enhanced in a quark gluon plasma if the temperature of the plasma is high enough, of the order of 500 MeV [20]. This will lead to an enhanced production of direct leptons from the semi-leptonic decay of charmed mesons formed during the hadronization phase. It is very unlikely that such high temperatures can be reached at SPS energies. Yet open charm is a very important observable which is not at all directly addressed in the present SPS program. A measurement of open charm will at least serve to check the extrapolation of the production from pp to pA and AA collisions; it will also provide a reference level for the future experiments at RHIC and LHC. The interest in such a measurement is further stimulated by the NA38 results [21]. They have noticed that the excess of dimuon pairs found in the intermediate mass region (see Section 1) has the same shape as the expected charm contribution, implying that an enhanced charm production (2 times bigger than expected) could be a possible explanation of the observed excess. The upgraded CERES spectrometer has potential features which can allow us to perform a direct measurement of the semileptonic decay of charmed mesons. The most attractive channels we are considering are $D^{\pm} \rightarrow K^{\mp}\pi^{\pm}e^{\pm}$ which have a $c\tau$ of 320 μm, (i.e. a decay length of several millimeters in the laboratory system). We capitalize on the excellent resolution of the silicon radial drift chambers and on the excellent electron identification of the RICH detectors, such that we can base the meson identification on a displaced vertex made by three tracks, one of them being an electron. We might also get some information on the charge and momentum of the π and the K by tracking them to the pad chamber located behind the spectrometer. Detailed simulations are being pursued at present to verify the feasibility of such an experiment.

4.3 Addition of an Electromagnetic Calorimeter

The mass resolution of the CERES experiment is limited to about 4% in the region of the ρ/ω. This is basically due to the design concept, i.e. the use of two RICH detectors with an upstream position of the associated UV counters, which inevitably implies a rather

low effective magnetic field integral. The addition of a high-precision electromagnetic calorimeter downstream of CERES with a momentum resolution of 1% and full coverage of the rapidity acceptance $2.0 < \eta < 2.6$ would allow to improve the mass resolution down to the 1% level and could also offer a number of other attractive features, e.g. in connection with π° and η detection, to further reduce the systematical errors in the direct photon program of CERES.

Such a calorimeter would need more than 5000 high-quality crystals like BaF_2 and would therefore be quite expensive. While this could hardly be justified with the CERES needs alone, a realistic possibility may develop in the future via the combination with HADES, a newly developed high-resolution dilepton spectrometer at GSI in Darmstadt which is presently under construction. An effort is being made during 1995, on a European scale, to develop for HADES a large BaF_2 calorimeter and to start raising the necessary funds. If this would converge, one could combine this with CERES for, e.g., one Pb beam time period in 1998 or 1999, analogous to the joint CERES/TAPS project which was successfully operated for several months of proton running during 1993.

5 Summary

The research program of CERES as proposed in ref. [2] has been substantiated and extended in three major aspects:

(i) Encouraged by the observation of a new source of dileptons of yet unexplained origin by CERES and other experiments in central sulphur collisions, an experimental effort to clarify its nature is called for.

(ii) The upgraded spectrometer was operated at the Pb beam in 1994 with implementation of new charged-particle tracking. The measured response of the detectors proves that the spectrometer can cope with central Pb-Au collisions and provide data samples of sufficient quantity and quality to study the new physics in the low-mass region.

(iii) With further improved data acquisition system also the intermediate mass range – where other degrees of freedom might manifest themselves – will become accessible within 2–3 years. A physics program for the more distant future includes a measurement at lower bombarding energy, reaching the highest baryon densities, and, if feasible, a study of charmed meson production through the semileptonic decay channels.

A Appendix: Results of the Pb Test Run and Completion of the Upgrade

In the first part of this appendix, we report on the experience gained with the upgraded spectrometer during the Pb test run in November 1994. We describe the running conditions, focus on the performance of the major components, i.e. the new vertex telescope of silicon drift detectors and the RICH detectors, and address the main points of concern expressed by the SPSLC: the vertex reconstruction, its efficiency, the number of hits in the RICH counters vs. event multiplicity, the close-pair rejection, and the ring reconstruction efficiency.

In the second part, we detail the necessary steps to complete the upgrade. This concerns mainly the completion of the data acquisition system (DAQ), the implementation of a new generation of silicon-drift detectors, and the pad chamber for tracking behind RICH-2. All those items will be ready for the run in 1995.

A.1 Results of the Pb Test Run

A.1.1 Running Conditions

Beam Line and Beam Counter

The CERES spectrometer is extremely sensitive to the beam conditions. This is mainly due to the large area of the UV detectors and to their high gain. Upstream interactions produce a large flux of charged particles which traverse the UV-detectors, in particular UV-1, adding a considerable load on them. To avoid upstream interactions as much as possible, no material is allowed along the beam path, and a vacuum pipe is used up to a few cm before the target. The only exception is a small gas Cherenkov beam counter, BC1 (17 cm of air with a thin mylar mirror), located 60 m upstream of the target (Fig. 4). A scintillator array (VW) of the size of UV-1 together with another scintillator (VC) located inside the vacuum pipe veto the residual upstream interactions, which can be be distinguished by time-of-flight from backward emitted particles of a target interaction.

Segmented Target

For the Pb runs we designed a new segmented Au target optimized to minimize the conversions and δ-electrons. The target is segmented into individual disks with a diameter of 600 μm and a thickness of 25 μm each. They are spaced by 3 mm such that on average only half a disk (12.5 μm, i.e. $X/X_0 = 0.37$ %) contributes to photon conversions within the acceptance of the spectrometer. We have used 8 disks, i.e. a total thickness of 200

μm of Au ($\lambda/\lambda_I = 0.83\%$) to limit the number of UV photons in RICH-1, originating from δ-rays produced by the Pb projectile on the target, to $\sim$25. Focusing the beam into this small target turned out to be a non-trivial operation. Several days of beam time were devoted to optimizing the collimators and magnet settings of the beam line. This took so long because the main Pb beam was accompanied by satellite Pb beams with an intensity reaching the percent level of the main beam, displaced by up to 5 mm. These satellite beams were hitting the silicon drift chambers creating a huge background in all detectors. After this unusual beam structure was found by performing a precise scan of the beam profile over a range of $\pm$1 cm, the problem was cured by a careful adjustment of the collimators.

First level trigger

The original setup of the first-level trigger (FLT) is completely changed; the principal concept, however, remains the same. The trigger is generated by the coincidence of a beam particle upstream and a minimum charged particle multiplicity downstream of the target. The layout is shown in Fig. 4.

The beam is tagged 60 m upstream of the target (BC1). The multiplicity information is obtained from a scintillator array of 24 identical azimuthal sectors (MD). It is located $\sim$6 m downstream of the target, covering the pseudorapidity region $2.9 < \eta < 4.7$. This range was chosen to minimize the amount of material in the MD acceptance. It is different from the acceptance of the spectrometer, $2.1 < \eta < 2.7$. However, since the particle rapidity distribution is symmetric around $\eta = 3$ in Pb-Au collisions, it triggers on the same particle density. Fig. 5 shows the correlation between the integrated analog pulse height of the MD vs. the number of hits in one of the silicon drift chambers for target interactions, and it clearly demonstrates that this simple scintillator array can effectively trigger on multiplicity. Interactions downstream of the target but in front of the multiplicity detector cannot be ignored when triggering at low multiplicities. In order to veto those interactions we will add a gas Cherenkov counter (BC3), right behind the target, which will recognize the beam particle.

Magnetic Field

During the whole test run, the spectrometer was operated with a magnetic field 22% higher than the design setting. This is one of the proposed steps [2] to improve the mass resolution. No technical problem was encountered.

Beam Intensity

There are three factors limiting the beam intensity: (i) safety considerations due to the radiation level in the environment, (ii) the overall load imposed on the UV-detectors from genuine target interactions, (iii) background hits in the UV-detectors produced by pile-up of beam particles within $\pm 2\mu s$ of the interaction.

The limit imposed by safety consideration was $\sim 10^6$/burst in 1994; we have adopted this beam rate for all estimates concerning the next two years. However, in the future we hope to run at intensities up to $5 \cdot 10^6$, and the maximum intensity tolerated in the H8 beam line needs to be investigated. In 1994 we have operated the experiment safely from 10^5 up to almost 10^6 ions/burst. Actually, the effective beam intensity was about a factor 3-4 higher due to a severe 50 Hz structure of the beam. We are therefore confident that the spectrometer can also be operated at several 10^6 ions/burst.

A.1.2 The Silicon Radial-Drift Chambers

The two silicon drift chambers (SIDC-1,2) are among the most important elements of the upgrade. They fulfill the following major tasks:

- The detectors allow for a vertex reconstruction free of ambiguities, due to their close spacing, which is still highly precise because the short lever arm is more than counterbalanced by the large number of tracks per event. The known vertex position allows to point into UV-1 to the centers of candidate rings. This *a priori* knowledge of ring centers reduces considerably the fake-ring probability, and it is a new feature of the 1994 set up. Previously, the whole detector area had to be searched for the presence of rings.

- The rejection of close pairs is greatly improved by the two-fold measurement of ionization for each track, as well as the recognition of close hits. This task is of prime importance for reducing the combinatorial background.

- The detectors provide also a very accurate off-line event characterization by the charged rapidity density $dn_{ch}/d\eta$, as they permit to correct for δ-rays and conversions.

The silicon drift chambers installed in the test run of 1994 were of the old 3"-diameter type. By adopting a revised production strategy it was possible to improve the radial symmetry of the drift field [3] – with dramatic consequences for the azimuthal hit

resolution. Laser tests performed in the laboratory showed excellent position resolution of better than 2 mrad in the azimuthal direction and of $\sim$20 μm in the radial direction.

We have successfully employed a new front-end electronics based on the 32-channel bipolar amplifier/shaper developed for ALICE [22] and accommodated to our requirements. The readout is fully based on complementary signals. This resulted in a complete removal of pickup allowing to set a low detection threshold. In addition, by increasing the drift field, the ballistic deficit with the new amplifier was reduced to about 20% over the full range of radial drift. Both measures will combine to overcome the loss in detection efficiency experienced in 1992 for hits in the inner part of the detector.

The doublet has an active inner and outer radius of 6 and 32 mm, respectively. It was mounted at an average distance of 9.3 cm downstream of the target, with a spacing of 1.4 cm between the two chambers, thus covering the pseudorapidity interval of $2.0 < \eta < 2.7$ for each of the 8 target disks. To increase the azimuthal track resolution, the two detectors are rotated with respect to each other by one-half anode pitch (0.5°).

Fig. 6 demonstrates the quality in the reconstruction of the interaction vertex without recourse to any sophisticated hit algorithm: the positions of the 8 disks of the segmented Au target are perfectly resolved along the beam line (left side of the figure); the lateral xy-position distribution of the reconstructed vertices (right side) reflects the folding of the beam profile with the extension of the target disks (600 μm diameter) indicated by the circle.

The vertex reconstruction efficiency is very high; more than 98% of the target interactions defined by the correlation between the multiplicity detector and the first silicon drift chamber as shown in Fig. 5, have a reconstructed vertex.

The local track resolution is displayed in Fig. 7. The values quoted in the figure represent the dispersion in SIDC-1 for tracks defined by the interaction vertex and a hit in SIDC-2. They result from the combined effect of the intrinsic resolution of the chambers, the vertex resolution and the multiple scattering. We notice the very good azimuthal resolution, considering the 17 mrad pitch of the anode structure, which results from the rotation of the two chambers and the charge sharing of the single hits among two anodes due to the diffusion.

A.1.3 The RICH Detectors

Readout Front-End Electronics of RICH-2

The front-end electronic modules of RICH-2 have been modified following the good experience gained with the second generation of UV-1 pad readout electronics, which was installed during 1992. The carrier boards which contain the preamplifiers are equipped with an improved protection circuit against sparks using low-leakage-current diodes, which ensure much better noise immunity. Analog-to-digital converter interfaces are directly connected onto the front-end modules. The pad amplitude signals are corrected for pedestal variations, digitized with 8-bit resolution and then transferred to the counting room. All the modifications were implemented prior to the 1994 run with Pb beams. As anticipated, they resulted in a reduction of the noise level and in a reduction of the total readout time from 1.5 ms in the old scheme to about 200 μs, thus making RICH-2 the fastest detector of the CERES setup.

Hits versus Multiplicity

Our first S-Au data taken in 1992 showed the expected linear dependence of the number of UV-photon hits in the RICH detectors with the charged particle rapidity density. In RICH-2 the hits were found to be in good agreement with the results of our general Monte Carlo simulations. In RICH-1 however, the measured slope was larger by about a factor of 1.7 compared to the simulations [3]. The origin of this discrepancy could not be clearly identified, although we suspected the unfavorable conditions of that beam time to be largely responsible for it. Lacking a convincing proof, we used the *measured* slope to extrapolate to central Pb-Pb collisions, in the simulations of our Pb proposal, which we considered to be a sufficiently safe approach. The hit multiplicity under the improved conditions of 1994 is therefore one of the key issues to be addressed with our first Pb data.

As part of our systematic endeavor to reduce background hits in the RICH detectors, we installed a W cylinder (16 cm long, 88 mm inner radius, and a thickness of 22 mm limited by the available space) around the target, to absorb the backward emitted particles. These are relatively slow particles; they deposit a large primary charge in the detectors giving rise to large hits or clusters which unnecessarily disturb the pattern recognition. In the short proton test beam period of 1994, we found that the W shield reduces the number of these clusters per interaction by almost a factor of three.

In Fig. 8 we show the number of hits in the two RICH detectors as a function of the charged particle pseudorapidity density as measured in SIDC-1 during the Pb-

beam period. The data display the expected linear dependence; there is an offset, more pronounced in RICH-1, which is mainly due to δ-electrons. The figure also shows the results of our general Monte Carlo simulations (solid line). The hit contributions from the various sources (conversions, π^0-Dalitz decays, pions, δ-electrons) in the simulation are separately indicated in the figure. We note that both RICH-1 and RICH-2 are in reasonably good agreement with the Monte Carlo results. Most significant, the slope in RICH-1 is now much smaller than the one measured in our run of 1992 with the S beam. This confirms the impression which was already apparent during the on-line event display that the central Pb-Au events look even nicer than our previous central S-Au events. We attribute this dramatic improvement to the combined effect of all the steps which were taken to reduce background hits and to ensure higher quality data: the installation of the W shield to absorb slow backward emitted particles, the installation, inside Radiator-1, of a better shielding against the Cherenkov photons generated by the passage of beam particles and forward pions outside the acceptance, a second generation of front-end electronics with much more stable performance in terms of noise and pedestal fluctuations, and finally a better algorithm to discriminate between highly ionizing particles traversing the UV detectors and single UV-photon hits.

A.1.4 Close Pair Rejection and Ring Efficiency

The combinatorial background originating from unrecognized partners of close pairs (photon conversions and π^0-Dalitz decays) is the main background source of the experiment. The amount of close pairs is largely suppressed by applying a $p_\perp$-cut of 200 MeV/c on the single electrons. In the original CERES setup, further rejection was achieved by the RICH detectors and the silicon drift detector [3]. In the upgraded spectrometer, the two silicon drift chambers play a decisive role together with RICH-1. All conversions occurring after the first silicon chamber are practically eliminated by requiring that every ring in RICH-1 is matched to a pair of hits in the two chambers. The amount of relevant conversions is then restricted to those occurring in the target and app. Half of those occurring inside the first silicon chamber. This amounts to a total radiation length of 0.55% such that the number of relevant conversions per event is practically equal to the number of π^0-Dalitz decays per event. This already represents an important improvement compared to the conditions of the S-Au run of 1992 where the total amount of material relevant for RICH-1 conversions was 2.35% of a radiation length. The relatively low level of remaining close pairs is further reduced by the pattern of the tracks defined by the

two silicon drift chambers together with the rings in RICH-1. Tracks are rejected if both silicon drift chambers show a double-d$E/$dx signal, or a close double hit, or if the ring in RICH-1 has a large enough amplitude. These criteria are of course correlated. Here we will quantify the rejection power of the doublet of silicon detectors only, which is the additional handle provided in the new scheme. The rejection based on the ring amplitude of RICH-1 is well documented in ref. [3].

Fig. 9 illustrates the results. The left side shows the correlation of the analog signals measured in the two silicon drift chambers from identified tracks; these are mainly single tracks, and the measured signals correspond to that of minimum ionizing particles. The right-hand side of the figure shows the same correlation for a sample of conversions identified in the RICH detectors by their typical V pattern: one ring in RICH-1 matched to two rings in RICH-2. A large class of about 60% of events with a double-d$E/$dx signal in both silicon chambers is clearly visible. One also sees a second class of events with a negligible signal in SIDC-1, corresponding to the late conversions. The fraction of those events is 22%. These figures demonstrate only part of the rejection power; the double-hit recognition will further improve it. Altogether, we expect the final rejection of close pairs to be at least as good as quoted in the Pb proposal [2].

The data taken with the Pb beam also allow us to reassess the ring reconstruction efficiency. This is best done by mixing a Monte-Carlo-generated electron track into a real event which is then passed through the whole analysis chain. The efficiency is determined by the ratio of reconstructed to generated tracks. In the proposal [2], lacking real data, the efficiency was determined using Monte-Carlo-generated events, based on an extrapolation of our S-Au data. This turned out to be a rather pessimistic approach for RICH-1 as the real events are in fact much cleaner, as discussed in the previous section. Consequently the revised ring reconstruction efficiency is higher in RICH-1, resulting in a slight improvement in the pair efficiency by a few percent from the value quoted in the proposal [2].

A.2 Completion of the Upgrade

A.2.1 Data Acquisition System and Readout Electronics

Another essential element of the upgrade is a new data acquisition system with a rate capability improved by about one order of magnitude compared to the system used in the sulfur run of 1992. This increase in overall speed is achieved by replacing the (slow) VMV bus used to accumulate the data from the detectors to form an event. We are now using a dedicated VME crate to collect the data for each event from the readout electronics of

all detectors in parallel into specially built memory modules at a rate of 50 MB/s. These memories are then read out by two CPUs via VME D64 blocktransfer at a measured speed of about 60 MB/s (including the overhead times to set up the transfer). In order not to compromise our extremely short Pb run in 1994, we did not exploit all the features of the new concept, in particular, we did neither try to optimize the timing nor to make use of the data compression available in the front-end electronic modules. In the time following the 1994 Pb run, we have continued to work on the completion and optimization of the DAQ hardware and software. With the measured performance achieved so far, together with the implementation of the data compression (using tables derived from the 1994 data) and further optimization of the total overhead time, the time to read out one event and store it in the event-buffer will be about 2 ms. Taking the dead time into account, the data acquisition system will be able to collect about 1000 events/burst with a total data volume of about 40 MB/burst. Using 3 DAT drives in parallel on each of two CPUs we have obtained transfer rates close to 3 MB/s, the theoretical limit for the chosen configuration. This rate is enough to match our needs; however, the concept enables an easy scaling in case of increased demands.

A.2.2 The Pad Chamber

The upgrade scheme includes the addition of a MWPC with pad readout located behind the spectrometer. Its main role is to help the pattern recognition of RICH-2 by providing an a priori knowledge of the ring-center location, thus reducing the fake-ring problem also in RICH-2. Since this problem is not as severe as in RICH-1, the pad chamber was not a 1994 item. The design has been completed following the concept described in ref. [2] with only two significant modifications: the wire anode will be manufactured in one piece, without radial spokes, thus eliminating losses inside the fiducial acceptance; the pad size will be exactly as in UV-2 chamber i.e 7.62 x 7.62 mm^2; this will allow us to use identical front-end electronic modules in the two chambers. The electrodes and housing of the pad chamber, its front-end electronics and the whole readout chain are under construction and are expected to be ready in time for the 1995 run. This schedule is on rather solid grounds as there is almost no development work involved, the pad chamber being a copy of existing elements in the CERES spectrometer.

A.2.3 The 4" Silicon Radial-Drift Chambers

A novel type of silicon radial-drift chambers based on 4" wafers had been designed at the end of 1993, and it came into production (Eurisys) in spring 1994. After the second round of production the first useful prototype became available. The fully mounted device arrived too late for thorough tests and was therefore not implemented for the Pb run in 1994. Presently, lithography masks, improved in minor details, are in preparation to start production along a revised scheme within the next month.

Besides a reduced hit density (due to a larger distance from the target) and the implementation of local charge injection for on-line calibration, the most important advantage of the new detectors derives from a novel split-anode structure, schematized in Fig. 10. The charge cloud is collected on five separate n implantations of different size, and the 8%-fractions received by the smallest electrodes are galvanically diverted to the neighboring channels on either side. By a recent laser test on the prototype, the proper functioning of this concept was demonstrated.

The split-anode structure will markedly improve the φ-resolution of a single detector as it enforces charge sharing also at short drift times. The resolution σ_φ of the doublet is expected to reach values below 1 mrad, and it will have an impact on the mass resolution of the spectrometer.

In addition to the detector development, an improved version of the front-end chip is presently being designed.

Rates and Sample Sizes

Table 1: Electron Pairs

target disks 8×25 μm Au	200 μm	
λ/λ_I	0.83%	
beam particles/burst (5 s/19 s)	$1 \cdot 10^6$	
60% on 600 μm Ø target	$6 \cdot 10^5$	
interactions/burst	5000	
dn/dy range	100 to 400	> 400
fraction of interactions	36%	7.5%
scaledown factor	3	1
first-level triggers/burst	600	375
total first-level triggers/burst	975	
DAQ lifetime (2 ms)	72%	
events to tape/burst	700	
$\langle dn/dy \rangle$	210	480
e^+e^-/event from hadronic sources	$2.8 \cdot 10^{-4}$	$6.5 \cdot 10^{-4}$
direct e^+e^-/event (enhancement 5)	$11 \cdot 10^{-4}$	$26 \cdot 10^{-4}$
events/30 days (100% run efficiency)	$5.6 \cdot 10^7$	$3.5 \cdot 10^7$
$\langle \epsilon_{pair} \rangle$	32%	16%
e^+e^--pairs from hadronic sources, $m_{ee} > 0.2$ GeV/c^2	5000	3600
total e^+e^--pairs (including direct source)	25000	19000
yield as a function of mass range:		
$0.20 < m_{ee} < 0.66$ (GeV/c^2)	17000	13000
$0.72 < m_{ee} < 0.84$ (GeV/c^2)	5400	3500
$0.94 < m_{ee} < 1.10$ (GeV/c^2)	850	550
$1.20 < m_{ee}$ (GeV/c^2)	400	300

Table 2: Direct Photons

target disks 8×25 μm Au	200 μm	
λ/λ_I	0.83%	
beam particles/burst (5 s/19 s)	$1 \cdot 10^6$	
interactions/burst	5000	
$dn/dy > 100$	2100	
DAQ lifetime (2 ms)	54%	
events to tape/burst	1100	
converter	1%	3%
conversions/event	1.3	3.9
$p_\perp > 60$ MeV/c	0.2	0.6
sample size (2 days each), $\langle \epsilon_{pair} \rangle = 50\%$	$9.5 \cdot 10^5$	$2.8 \cdot 10^6$

References

[1] U. Faschingbauer et al., CERES Collaboration, Proposal to the SPSC, CERN SPSC/88–25/P237 and SPSC/88–40/P237/Add 1

[2] H. Kraner et al., CERES Collaboration, Proposal to the SPSLC, CERN SPSLC/94–1/P280

[3] CERES/NA45 Status Report to the SPSLC, CERN/SPSLC 94-2, SPSLC/M529.

[4] R. Baur et al., (Proc. First Workshop on RICH Detectors, Bari 1993), Nucl. Instr. Meth. **A343** (1994) 87

[5] W. Chen et al., IEEE Trans. Nucl. Sci. **NS-39** (1992) 619

[6] E.V. Shuryak, Phys. Lett. **78B** (1978) 150, Sov. J. Nucl. Phys. **28** (1978) 408

[7] P.V. Ruuskanen in: Quark-Gluon-Plasma – advanced series on directions in high energy physics, Vol. 6. R. Hwa (ed.), Singapore, World Scientific 1990

[8] K. Kajantie et al., Phys. Rev. **D34** (1986) 2746

[9] R. Baur et al., CERES Collaboration, Phys. Lett. **B332** (1994) 471

[10] T. Akesson et al., HELIOS/1 Collaboration, CERN–PPE/94–140, submitted to Z. Phys. **C**

[11] G. Agakichiev et al., CERES Collaboration, submitted to Phys. Rev. Lett.

[12] P. Wurm, CERES Collaboration (Quark Matter 95, Proc. Int. Conf. on Ultra-Relativistic Nucleus-Nucleus Collisions, Monterey 1995), to appear in Nucl. Phys.

[13] M. Masera, HELIOS/3 Collaboration, ibid.

[14] I. Tserruya, ibid.

[15] P.V. Ruuskanen, Nucl. Phys. **A544** (1992) 169c

[16] J. Cleymans, V.V. Goloviznin, R. Redlich, Z. Phys. **C59** (1993) 495

[17] R. Pisarski, Phys. Lett. **B110** (1982) 155

[18] D. Irmscher, CERES Collaboration (Quark Matter 93, Proc. Int. Conf. on Ultra-Relativistic Nucleus-Nucleus Collisions, Borlänge 1993), Nucl. Phys. **A566** (1994) 347c

[19] T. Awes, WA80 Collaboration (Quark Matter 95, Proc. Int. Conf. on Ultra-Relativistic Nucleus-Nucleus Collisions, Monterey 1995), to appear in Nucl. Phys.

[20] A. Shor, Phys. Lett. **B215** (1988) 375 and Phys. Lett. **B233** (1989) 231

[21] M.C. Abreu et al., NA38 Collaboration (Quark Matter 93, Proc. Int. Conf. on Ultra-Relativistic Nucleus-Nucleus Collisions, Borlänge 1993), Nucl. Phys. **A566** (1994) 77c

[22] W. Dabrowski et al., ALICE internal report, CERN 1994

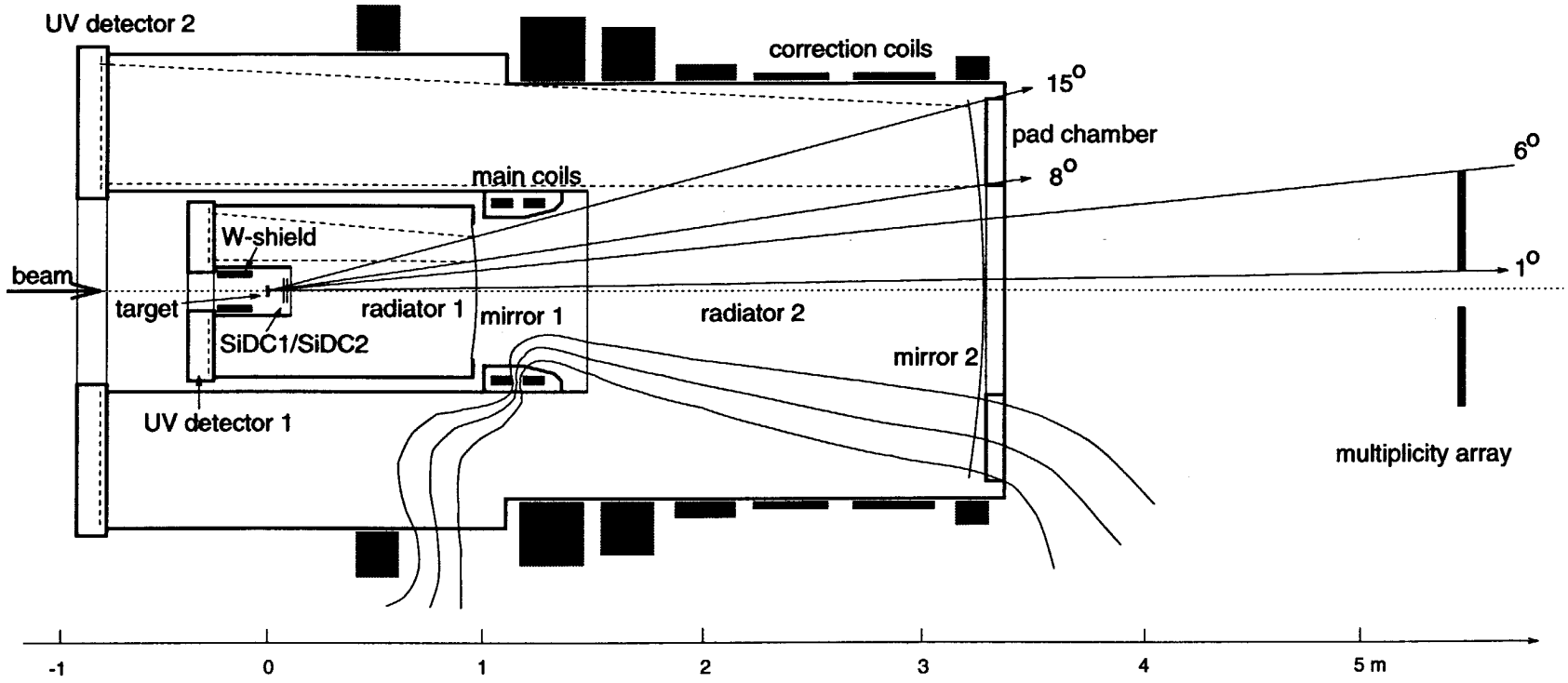

Figure 1: Setup of the CERES spectrometer for Pb beam

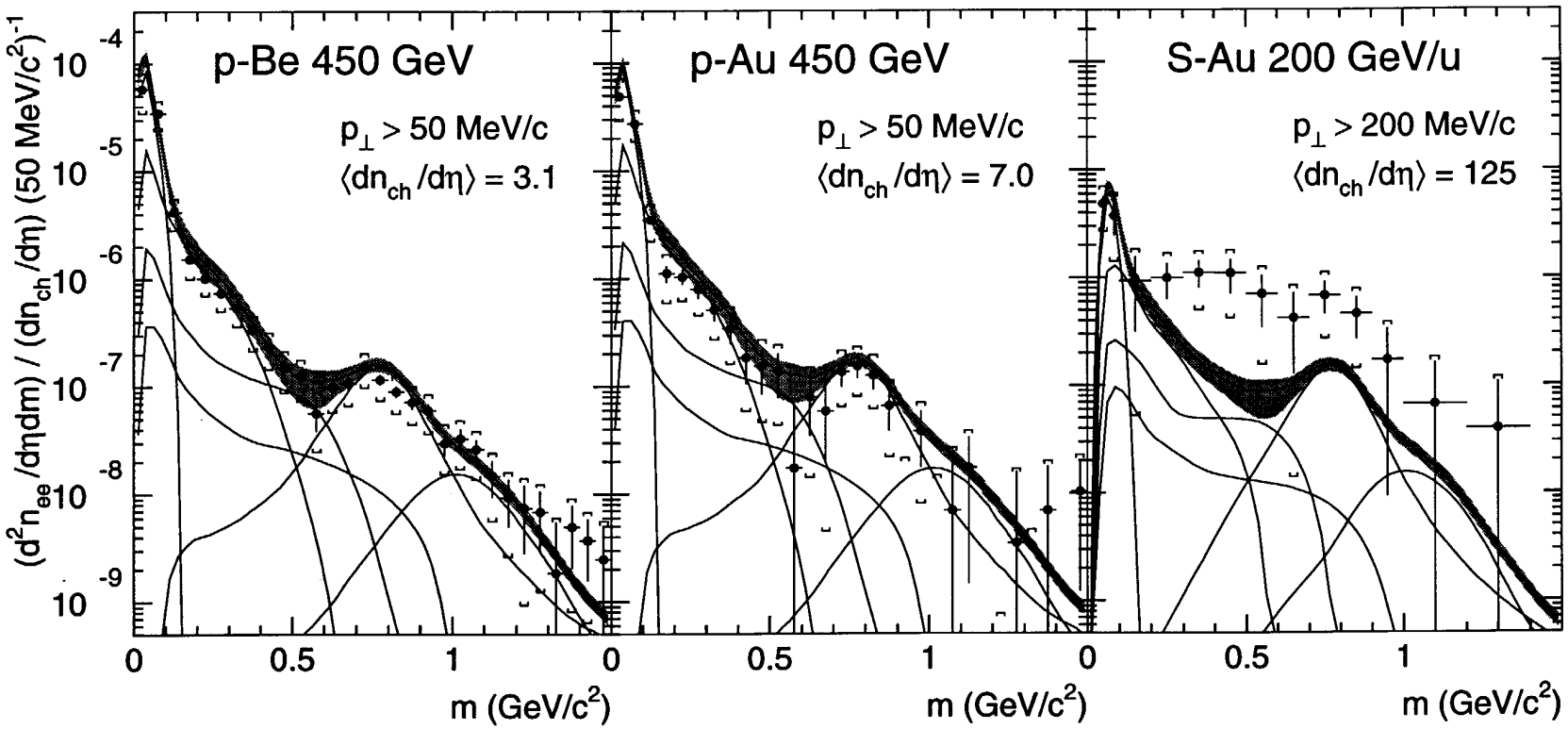

Figure 2: Invariant-mass spectra measured by CERES for the collision systems p-Be, p-Au and S-Au. The average charged-particle densities used in the normalization are quoted in the figure. The statistical errors are shown as bars, the brackets denote the systematic errors added linearly to the statistical ones.

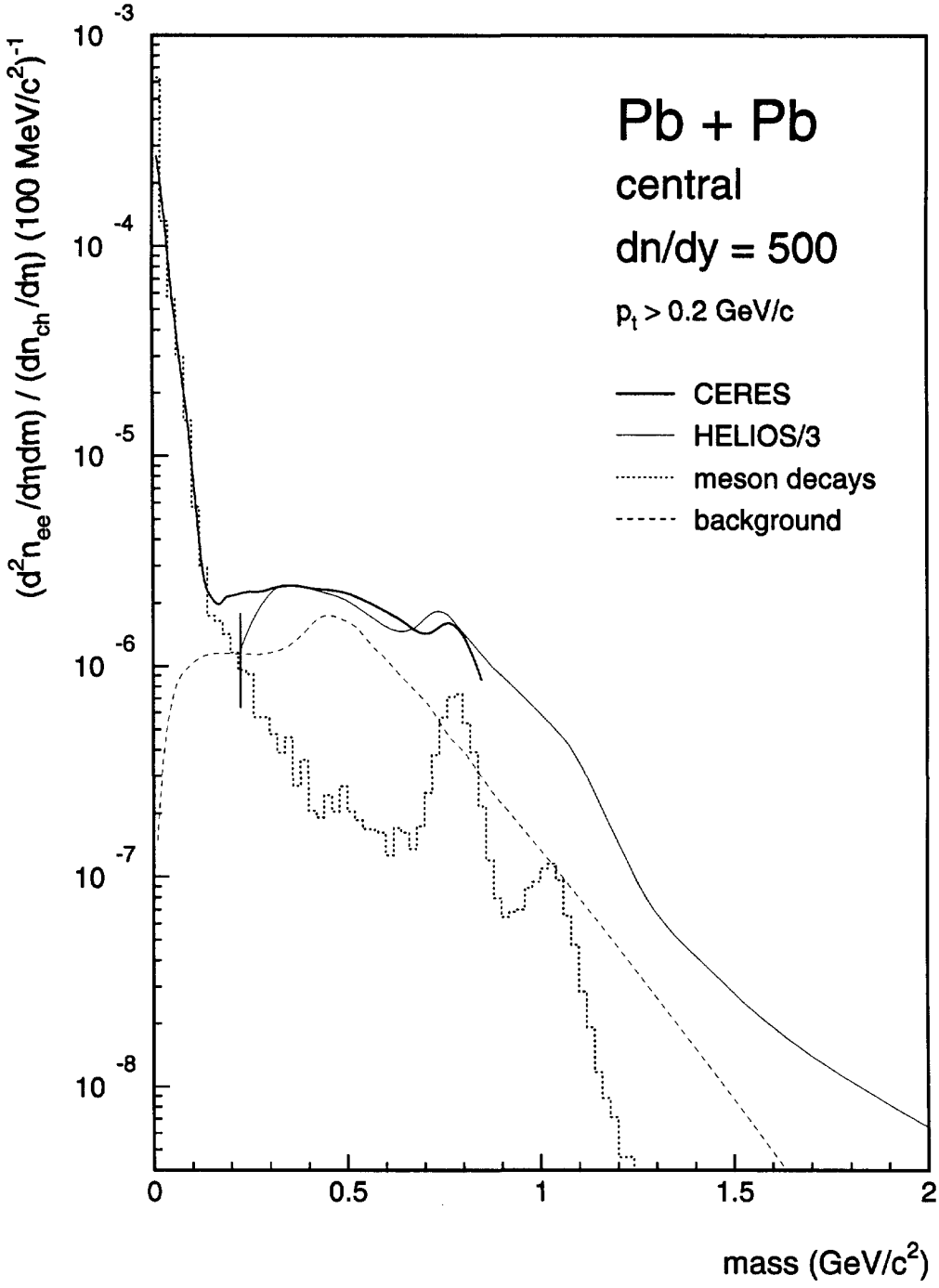

Figure 3: Yield of electron pairs per charged particle for central Pb-Pb collisions vs. invariant mass as expected from the enhancement factor of 5 measured by CERES for S-Au in the low-mass region (thick solid line). The yield of the dimuons measured by HELIOS/3 for S-W has been set on scale to display the same enhancement in the low-mass region (thin solid line) and allows to extend the expected shape to higher masses. The hadronic contributions (dotted histogram) contain no resonances heavier than the ϕ and are folded with the CERES acceptance and mass resolution. The same holds for the Monte Carlo simulated combinatorial background (dashed line).

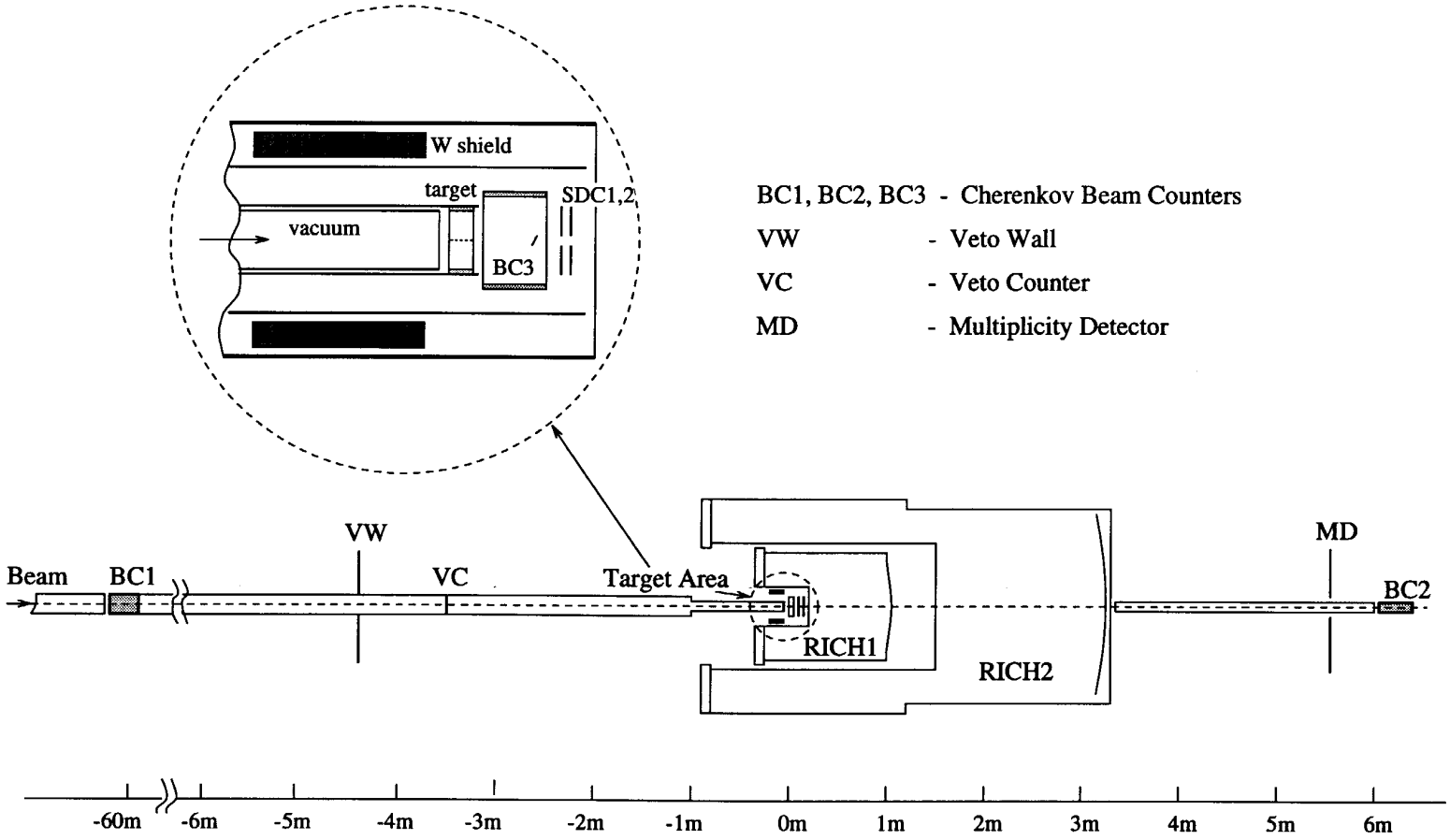

Figure 4: The first-level trigger layout for Pb beam

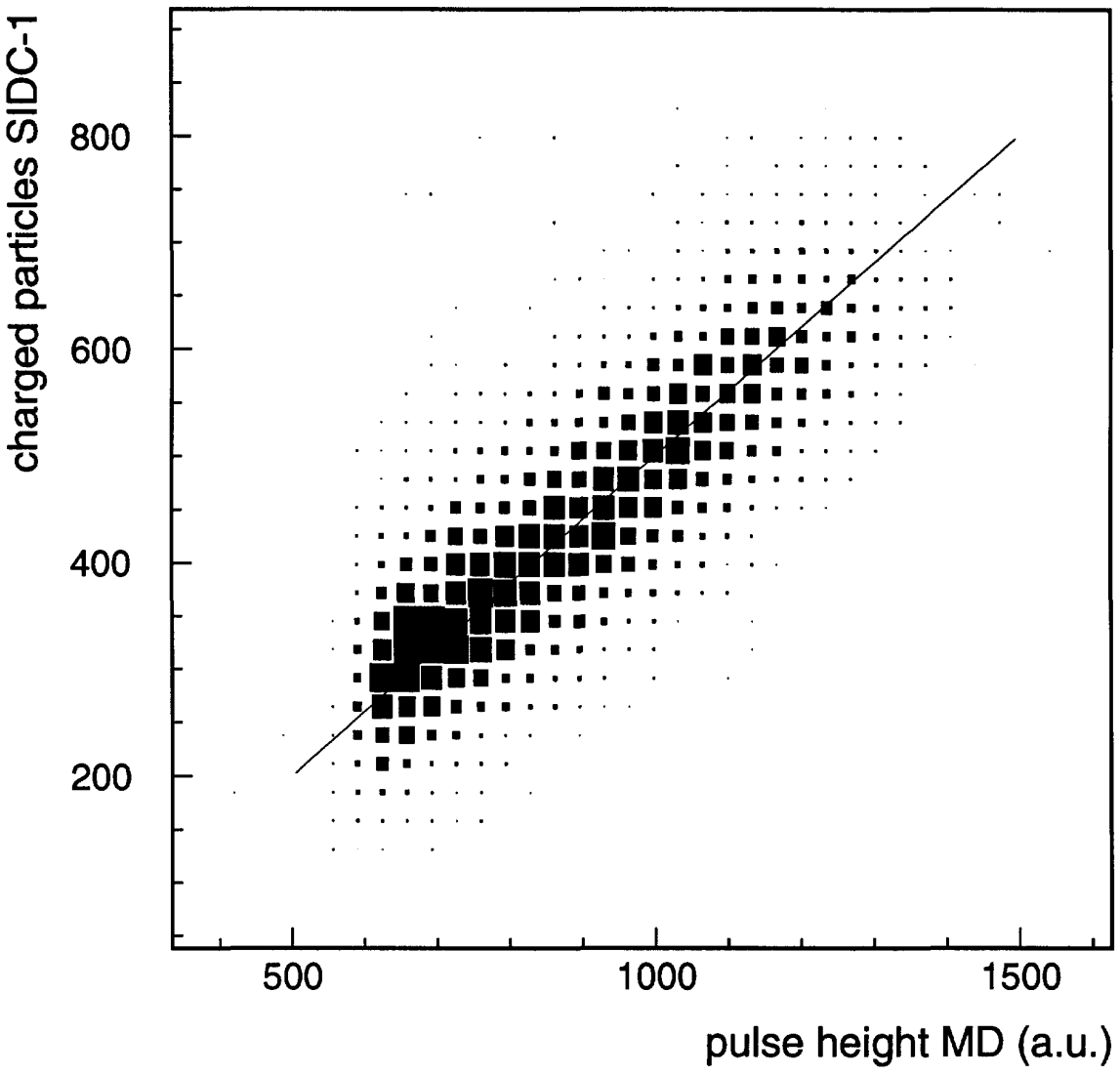

Figure 5: Correlation of the integrated pulse height measured by the multiplicity array MD and the hit multiplicity in SIDC-1 for events with a reconstructed interaction vertex in the target

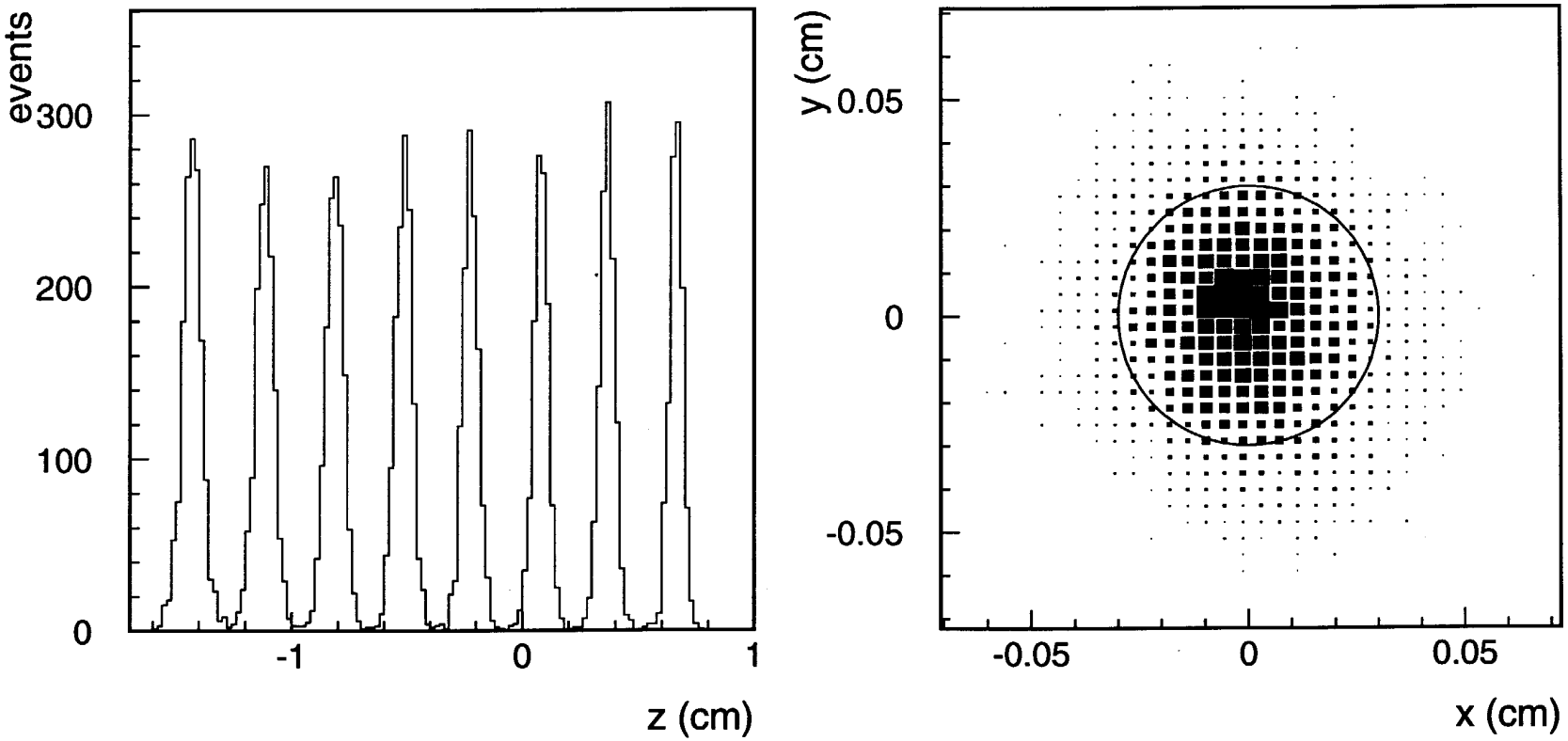

Figure 6: Determination of the interaction vertex with the doublet of silicon drift chambers: distribution of reconstructed vertex positions *along* the beam axis showing the resolved 8 Au target disks of 25 μm thickness each (left), and the distribution of the *lateral* xy-position of the reconstructed vertices (right), reflecting the beam profile folded with the target disks of 600 μm diameter (marked as a circle) and the reconstruction resolution.

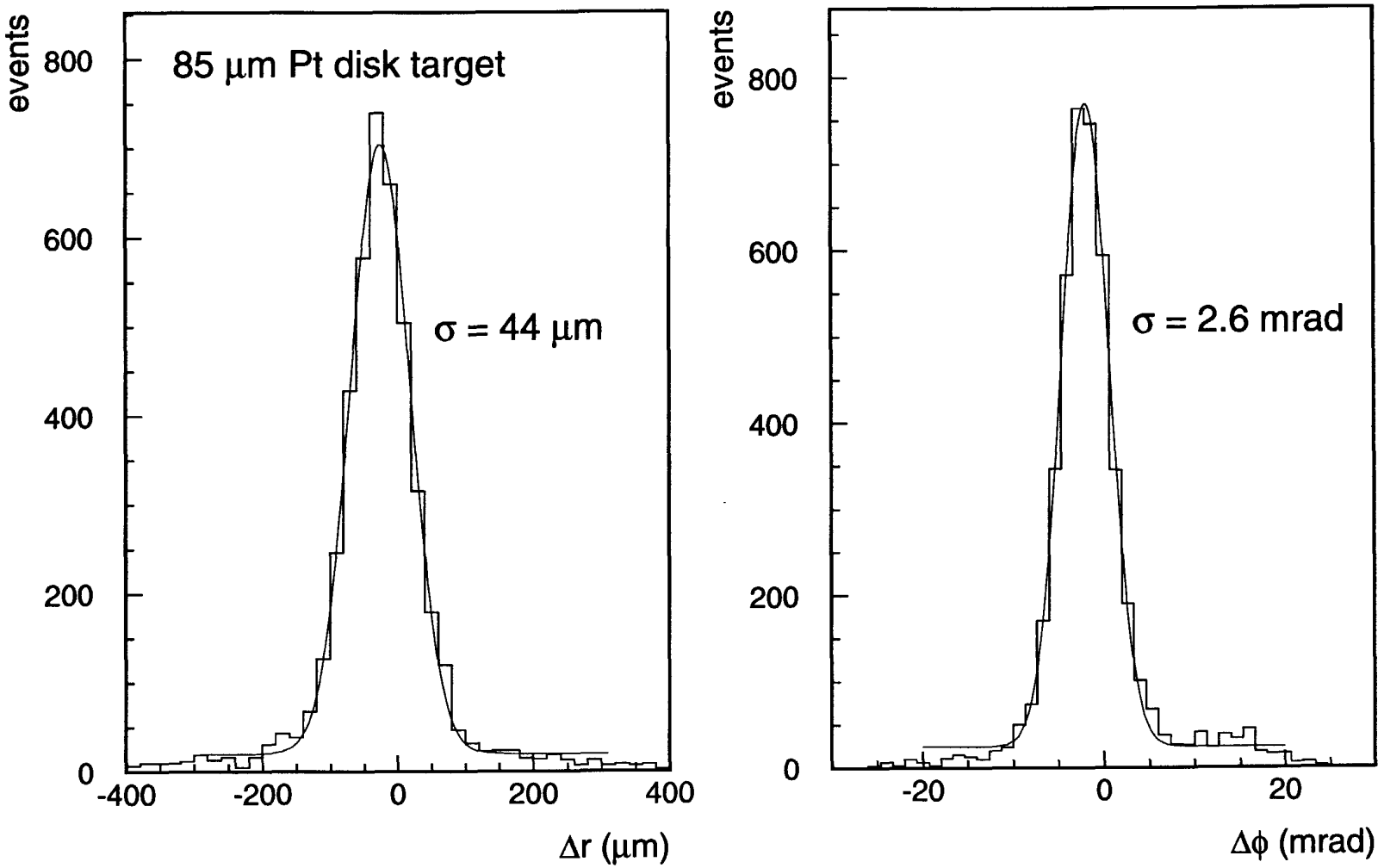

Figure 7: Local track accuracy of the silicon drift chambers: radial and azimuthal residuals in SIDC-1 for tracks defined by the interaction vertex and a hit in SIDC-2.

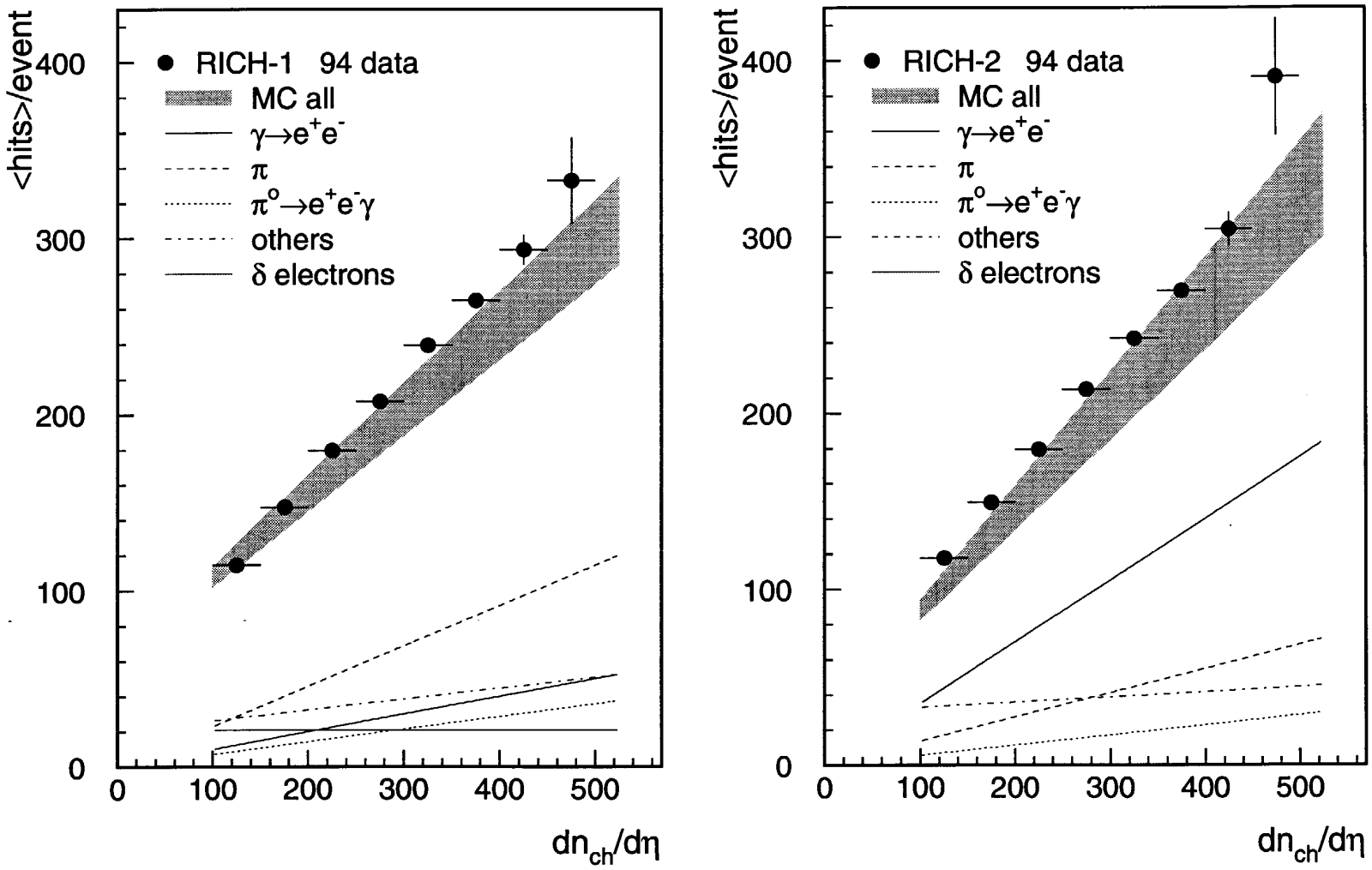

Figure 8: Mean number of hits per event vs. charged particle pseudorapidity density in RICH-1 and RICH-2 for Pb-Au interactions. The band represents the number of hits per event from Monte Carlo simulations; its width shows the present systematic errors, including those from the multiplicity scale.

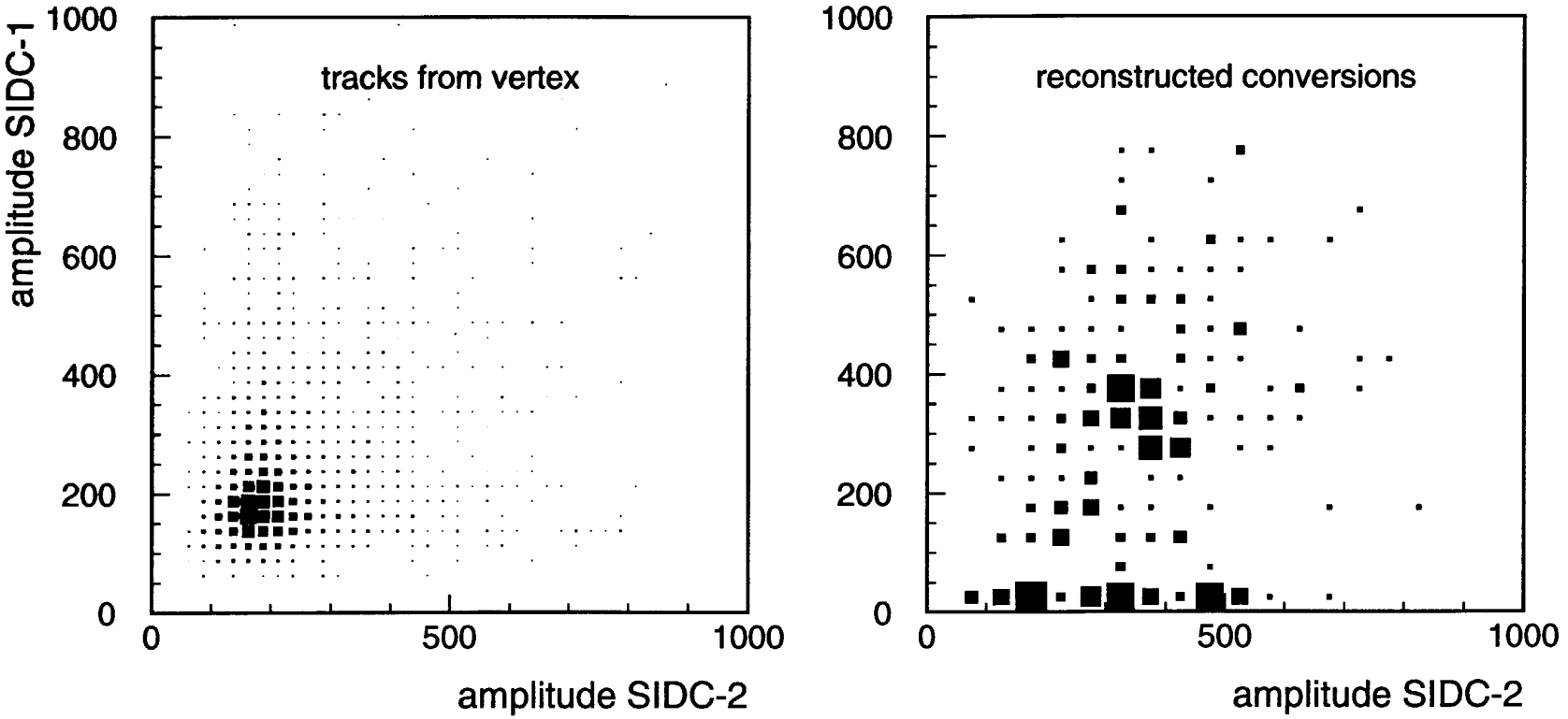

Figure 9: Distributions of $\mathrm{d}E/\mathrm{d}x$ in SIDC-1 vs. SIDC-2 for all tracks pointing to the vertex (left), and for a sample of reconstructed conversions (right), exhibiting double-$\mathrm{d}E/\mathrm{d}x$.

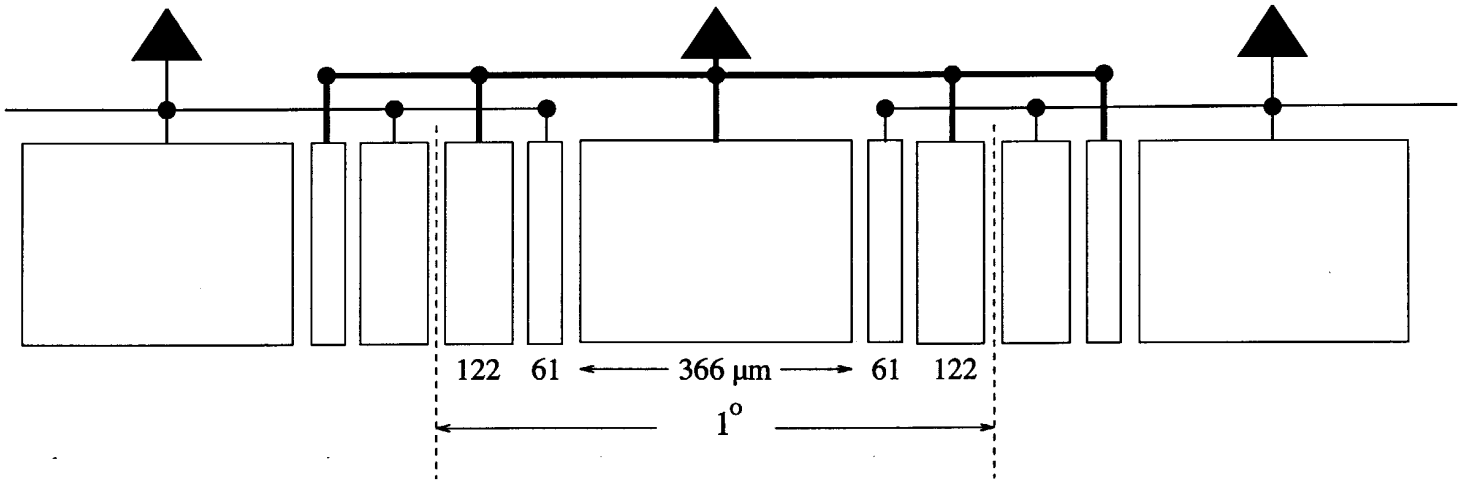

Figure 10: Split anode structure of the new 4" silicon drift chambers. To improve azimuthal resolution, the charges collected by the 360 readout channels receive small contributions from electrodes belonging to adjacent anodes

EUROPEAN ORGANIZATION FOR NUCLEAR RESEARCH

CERN–PPE/95–??
March 19, 1995

ENHANCED PRODUCTION OF LOW-MASS ELECTRON PAIRS IN 200 GeV/u S-AU COLLISIONS AT THE CERN-SPS*

G. Agakichiev[1,c)], R. Baur[2)], A. Breskin[3)], R. Chechik[3)], A. Drees[2)], C. Jacob[1)], U. Faschingbauer[1)], P. Fischer[2)], Z. Fraenkel[3)], Ch. Fuchs[1)], E. Gatti[4)], P. Glässel[2)], Th. Günzel[2)], C. P. de los Heros[3)], F. Hess[1)], D. Irmscher[2)], B. Lenkeit[2)], L. H. Olsen[2)], Y. Panebrattsev[1,c)], A. Pfeiffer[2)], I. Ravinovich[3)], P. Rehak[5)], A. Schön[2)], J. Schukraft[6)], M. Sampietro[4)], S. Shimansky[6,c)], A. Shor[3)], H. J. Specht[2)], V. Steiner[3)], S. Tapprogge[2)], G. Tel-Zur[3)], I. Tserruya[3)], Th. Ullrich[2)], J. P. Wurm[1)], V. Yurevich[6,c)]

(CERES Collaboration)

Abstract

We report on measurements of low-mass electron pairs in 450 GeV p-Be, p-Au and 200 GeV/u S-Au collisions at central rapidities. For the proton induced interactions, the low-mass spectra are, within the systematic errors, satisfactorily explained by electron pairs from hadron decays, whereas in the S-Au system an enhancement over the hadronic contributions by a factor of $5.0 \pm 0.7(\text{stat.}) \pm 2.0(\text{syst.})$ in the invariant mass range $0.2 < m < 1.5$ GeV/c^2 is observed. The properties of the excess suggest that it arises from two-pion annihilation $\pi\pi \rightarrow e^+e^-$.

(Submitted to Physical Review Letters)

[1)] Max-Planck-Institut für Kernphysik, 69117 Heidelberg, Germany
[2)] Physikalisches Institut der Universität Heidelberg, 69120 Heidelberg, Germany
[3)] Weizmann Institute, Rehovot 76100, Israel
[4)] Politecnico di Milano, 20133 Milano, Italy
[5)] Brookhaven National Laboratory, Upton, NY 11973, USA
[6)] CERN, 1211 Geneva 23, Switzerland
[c)] visiting from JINR, Dubna, Russia

Quantum Chromodynamics predicts at very high densities and temperatures a phase transition from ordinary hadronic matter to a quark-gluon plasma, i.e., a state where quarks and gluons are not confined to hadrons. The energy densities achieved in fixed-target heavy ion collisions at the CERN SPS are considered to be sufficiently high to reach such a phase transition. The ultimate motivation of the ongoing program is to put the conjectured plasma state to a stringent test and to learn about its properties.

The production of lepton pairs is commonly accepted as a promising probe to study the dynamical evolution of nuclear collision processes [1]. Leptons interact only electromagnetically and their mean free path is considerably larger than the transverse size of the collision volume. They are produced during the entire space time evolution of the system, beginning at the early hot stage up to the point where the hadrons cease to interact. Later, a large amount of additional lepton pairs is produced by the electromagnetic decays of hadronic particles. Since all stages of the collision have somewhat different contributions to the lepton spectrum, a careful analysis should, in principle, be able to unfold the whole space time history of the hadronic collision, including contributions both from the quark (via $q\bar{q}$-annihilation) and the hadronic phase (via $\pi\pi$-annihilation) [2, 3, 4, 5].

Up to now, two experiments have succeeded in measuring dimuons in heavy ion collisions at the CERN SPS, one at high masses [6], the other also in the low-mass range [7]. We present here the results of the first measurement of low-mass electron pairs in S-Au collisions taken with the CERES/NA45 spectrometer and compare them with those from p-Be and p-Au collisions obtained with the same apparatus. The systematic study from pp up to heavy nuclear systems is essential to (i) understand the production level in ordinary hadronic collisions and (ii) to identify any possible deviations from the mere superposition of pp collisions.

Our main results can be summarized as follows: low-mass electron pairs produced in proton induced reactions can, within the systematic errors, be accounted for by pairs from the decay of hadrons, whereas in S-Au collisions a strong enhancement over the hadronic contributions is observed in the invariant mass range $0.2 < m < 1.5$ GeV/c^2.

CERES (Fig. 1) is an experiment dedicated to the measurement of low-mass electron pairs. The acceptance covers the pseudorapidity region $2.1 < \eta < 2.7$ and the invariant mass range from 50 MeV/c^2 to beyond 1 GeV/c^2. A detailed description of the CERES/NA45 experiment can be found in [8]. Here we summarize the most relevant features of the detector. Particle identification and directional tracking are based on two azimuthally symmetric RICH detectors with a Cherenkov threshold ($\gamma_{th} \simeq 32$) high enough to substantially suppress signals from the large number of hadrons produced in the collision. A superconducting double solenoid between the two detectors provides an azimuthal deflection for momentum determination, leaving the polar angle θ unchanged. The magnetic field (sketched in Fig. 1) in the region of the inner RICH radiator is compensated to nearly zero using an asymmetry in the currents of the coils, thus preserving the information of the original direction of the particles. A set of correction coils shapes the field in the second RICH radiator such that it points back to the target, ensuring straight trajectories and therefore sharp ring images. The Cherenkov photons from the RICH radiators are registered in two UV-detectors which are placed upstream of the target and are therefore not subject to the large flux of forward going charged particles. The information of the detectors is read out via two-dimensional arrays of about 50000 pads each, allowing the unambiguous reconstruction of single photon hits.

A novel radial-drift silicon detector with 360 charge-collecting anodes on the outer perimeter of a 3" wafer [9] situated closely behind the target is used for high-resolution

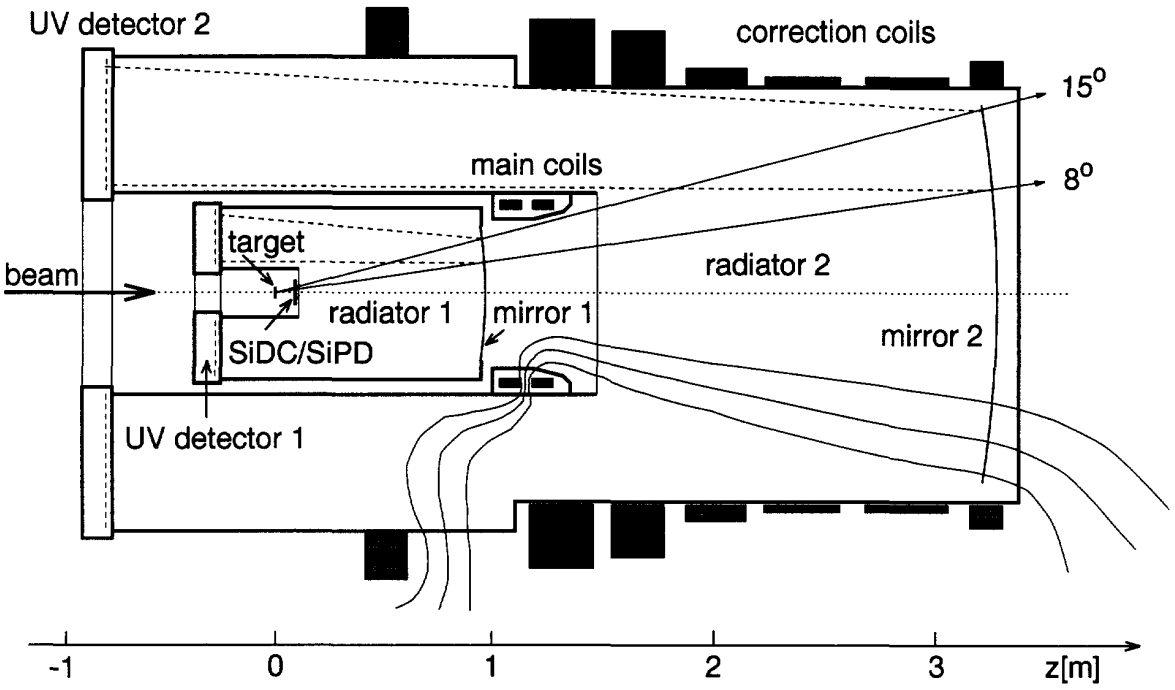

Figure 1: Schematic view of the CERES spectrometer.

vertex reconstruction and tracking. Its prime purpose is to supply additional rejection of photon conversions and Dalitz pairs which is necessary for a sufficient reduction of the combinatorial pair background in nucleus-nucleus collisions. An additional silicon pad detector [10] segmented into 64 pads supplies information about the charged-particle multiplicity both for first-level triggering and off-line analysis.

The S-Au results described in this report were obtained from the analysis of data taken during the SPS fixed-target running period in the spring of 1992. A total of $3.6 \cdot 10^6$ first-level and $2.7 \cdot 10^6$ second-level triggers were recorded. The first-level trigger uses the analog information from the silicon pad detector to select events in a wide multiplicity range with an average multiplicity of $\langle dn_{ch}/d\eta \rangle = 125$ in the overall data sample. The second-level trigger is formed by a systolic processor array [11] which searches for distant pairs of Cherenkov rings while suppressing the background of close pairs ($\theta_{ee} < 35$ mrad) from π^0-Dalitz decays and conversions. Since the original opening angle of the pairs is indispensable for this operation only the data from the first RICH detector is used in the trigger.

The p-Be and p-Au data were taken in summer 1993. In addition to the setup for the sulphur beam, a fast intermediate-level trigger [8], based on a more restricted subsample of the inner RICH detector data, was used to further enhance the open pair signal, resulting in an overall enrichment factor of $\sim$175 and $\sim$75 for p-Be and p-Au, respectively. The data samples correspond to $2.1 \cdot 10^9$ minimum bias events in p-Be and $2.7 \cdot 10^8$ in p-Au collisions.

The off-line electron reconstruction is very similar in almost all aspects for p-Be, p-Au and S-Au events. A pattern-recognition algorithm reconstructs ring images without the prior knowledge of the Cherenkov ring centers. In the first step, electronic noise and clusters from highly ionizing particles traversing the photon detectors, which would otherwise confuse the ring reconstruction, are eliminated. Ring candidates are then iden-

tified using a Hough transformation on the remaining picture. In the vicinity of these candidates, single-photon hits are reconstructed and used to determine the position of the rings by a fitting procedure. Various ring quality criteria are applied to distinguish genuine Cherenkov rings from fake rings originating from random combinations of hits. For the S-Au data sample, these cuts are performed by a neural network algorithm in order to optimize the efficiency of the decision. The accepted rings in both RICH detectors are then combined to tracks, identified by their common angle θ with respect to the beam axis. Two tracks sharing the same unresolved double ring in the first RICH detector are rejected as photon conversion candidates. The remaining tracks are combined into pairs.

The combinatorial background originating from unrecognized partners of low-mass Dalitz and conversion pairs is *the* central problem of the experiment, and is the only significant source of physics background. Due to the fact that the inclusive electron spectrum from π^0-Dalitz decays and conversions is considerably softer than that of pairs with $m > 0.2$ GeV/c^2, the signal-to-background ratio (S/B) can be significantly improved by a $p_\perp$-cut on the single electrons. The results discussed here are presented with a $p_\perp$-cut of 200 MeV/c for the S-Au data. Due to the lower background in proton induced collisions ($S/B \propto 1/n_{ch}$) a looser $p_\perp$-cut of 50 MeV/c has been chosen for the p-Be and p-Au sample. Further rejection cuts, most of them exploiting the small opening angle of the low-mass pairs, are applied to improve the S/B ratio. The most important are: a close-ring cut in the first RICH to remove π^0-Dalitz and conversion pairs with unrecognized partners in the second RICH, a total ring-amplitude cut to reject unresolved double rings, and cuts on the match quality to the silicon drift chamber to eliminate conversions after the silicon detector and tracks not originating from the target. Although the S/B ratio in p-Be and p-Au collisions also improves by the use of the silicon drift detector, the pair signal itself decreases by a factor of two due to imperfections of the hardware; it was therefore not used in the analysis of the proton-nucleus data. In the S-Au data sample, however, its rejection power was essential due to the much smaller initial S/B ratio.

The combined effect of all cuts results in an improvement of the S/B ratio by one order of magnitude. In order to minimize the influence of the second-level trigger bias, only pairs with opening angles $\theta_{ee} > 35$ mrad are taken into account. The remaining combinatorial background in the e^+e^--sample is determined by the number of like-sign pairs. The pair signal S is then extracted by subtracting the like-sign contribution from the e^+e^--sample as $S = N_{+-} - 2\,(N_{++}\,N_{--})^{1/2}$.

The final S-Au sample for $m > 0.2$ GeV/c^2 consists of 4249 pairs of which 2346 are e^+e^-, resulting in a net pair signal of 445 ± 65 with a S/B ratio of 1/4.3, while in the high-statistics p-Be (p-Au) sample a signal of 5760 ± 184 (1126 ± 100) pairs is obtained at a S/B ratio of 1/2.2 (1/4.5).

In the absence of *new* physics, the main sources of electron pairs are expected to be hadron decays [12]. For pair masses below 140 MeV/c^2, the π^0-Dalitz decay dominates the spectrum, whereas at higher masses the decays $\eta \to e^+e^-\gamma$, $\omega \to e^+e^-\pi^0$ and $\rho/\omega \to e^+e^-$ should be the most significant. We have calculated the invariant-mass spectrum with a generator containing all known hadronic sources, i.e., the π^0, η, η', ρ, ω and ϕ. Their $p_\perp$-distributions were generated assuming $m_\perp$-scaling [13] based on pion $p_\perp$-spectra from different experiments [14, 15, 16]. The rapidity distribution for pions was a fit to measured data [17] for S-Au which was modified for the heavier mesons to reflect the respective ratio of $\sigma_{central}/\sigma_{tot}$ as measured by NA27 [18] for pp; the relative rapidity densities for the various mesons were also taken from ref. [18]. All Dalitz decays were treated according to the Kroll-Wada expression with the experimental transition form factors taken from ref.

[19]; the vector meson decays were generated using the expressions derived by Gounaris and Sakurai in ref. [20]. Charm production was not taken into account since it is negligible in the low-mass range. Finally, the laboratory momenta of the electrons were convoluted with the experimental resolution and acceptance.

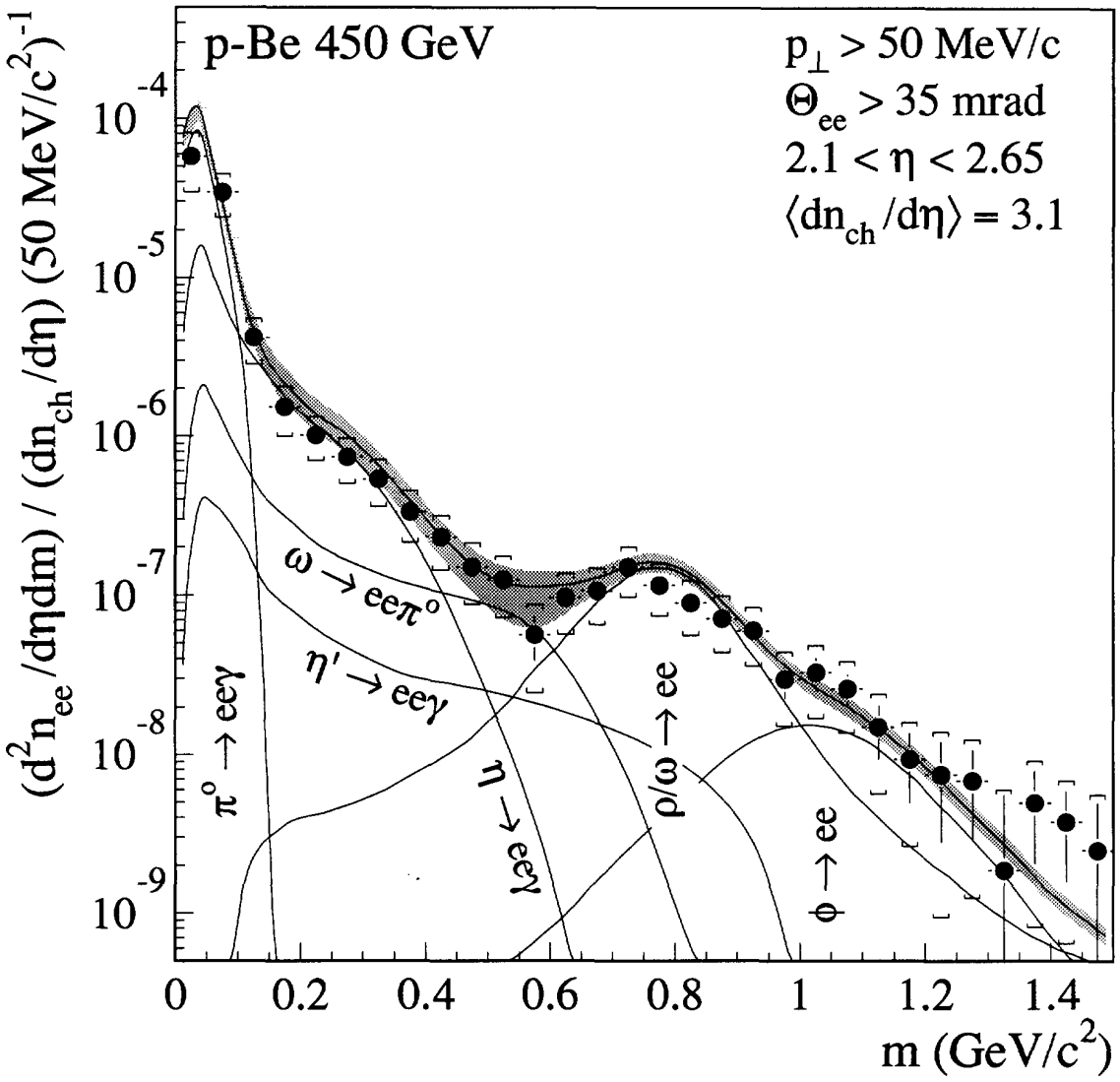

Figure 2: Inclusive e^+e^- mass spectra in 450 GeV p-Be collisions showing the data (full circles) and the various contributions from hadron decays. The shaded region indicates the systematic error on the summed contributions. No pair-acceptance corrections are applied.

The results for the p-Be, p-Au and S-Au data samples are shown in Figs. 2, 3 and 4. All three spectra are normalized to represent *pair density per charged-particle density* within the rapidity acceptance $2.1 < y < 2.65$; the average charged particle densities used in the normalization are quoted in the figures. The statistical errors are marked by bars, whereas the brackets reflect the systematic uncertainties due to reconstruction efficiency, acceptance and trigger enrichment, linearly added to the statistical errors.

The various contributions from hadron decays for the respective colliding systems are shown in all three figures. The shaded region indicates the systematic error on the

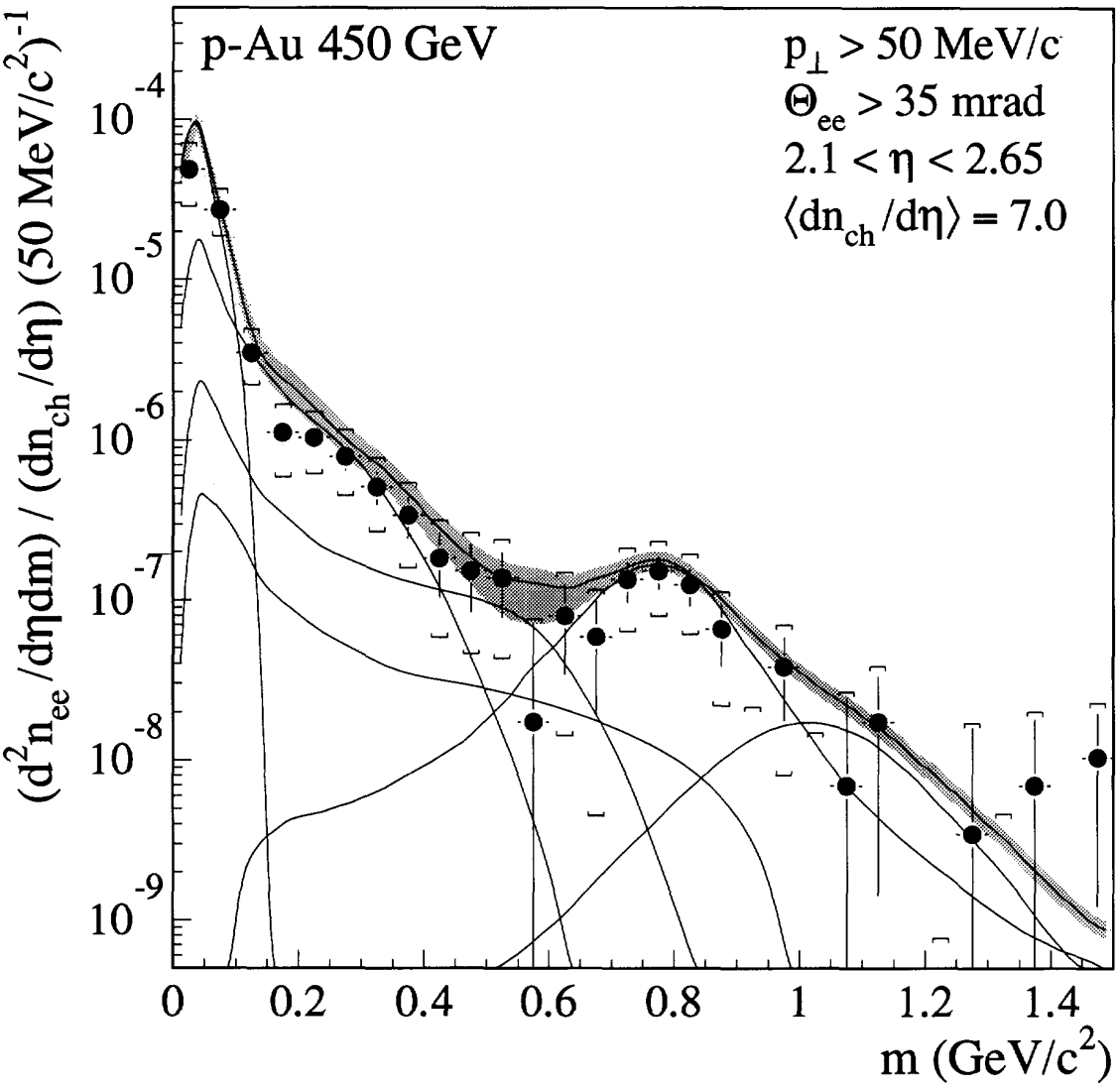

Figure 3: Inclusive e^+e^- mass spectra in 450 GeV p-Au collisions.

total contribution from hadron decays. The data and the predictions are *not* corrected for pair acceptance (i.e., the ratio of the geometrical acceptances of the virtual photon to the two tracks of the pair), since this correction would require deeper knowledge of all sources of pairs, which obviously does not yet exist for the S-Au case.

For both the p-Be and the p-Au sample, the measured inclusive e^+e^--pair spectra are well explained, within the present systematic errors, by electron pairs from hadron decays, and there is no need to invoke any unconventional source as also reported previously in ref. [12]. In the S-Au data sample, however, a statistically significant enhancement is observed. As a quantitative measure of the observed excess we define the enhancement factor as the integral of the data over the integral of the predicted sources in the mass range $0.2 < m < 1.5$ GeV/c^2 which results in 5.0 ± 0.7(stat.)± 2.0(syst.). A striking feature of the S-Au spectrum is the absence of any enhancement for masses below approximately 250 MeV/c^2. A second independent analysis gives essentially the same results [21].

If the observed excess originates from collective processes in a thermalized system it should vary as the square of the charged-particle density. Although quantitative studies of

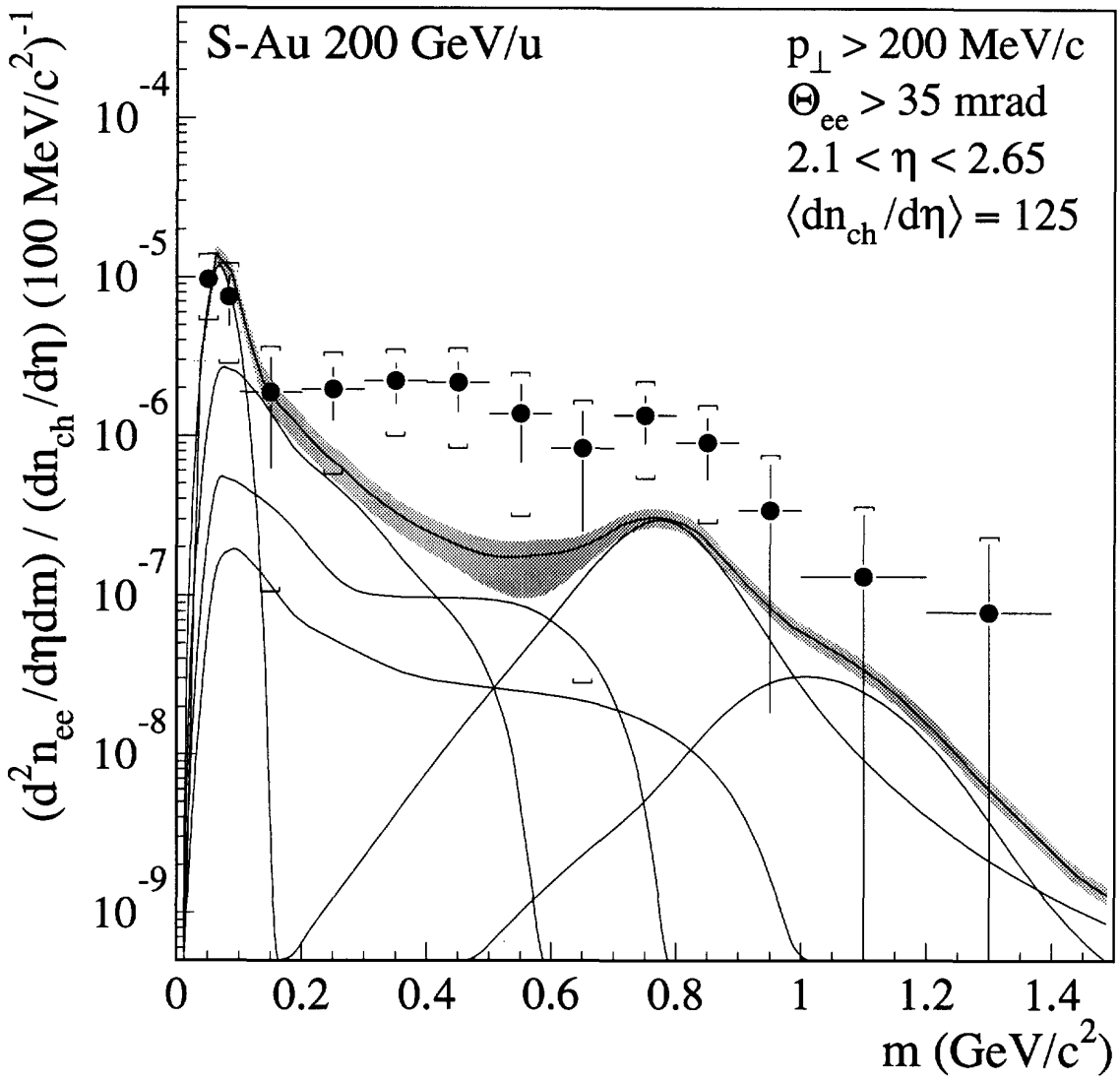

Figure 4: Inclusive e^+e^- mass spectra in 200 GeV/u S-Au collisions.

this characteristic behavior suffer from the limited statistics of our S-Au data sample one can derive an indication of a quadratic dependence by comparing our data with results obtained by the HELIOS/3 collaboration, also reporting an excess production of dileptons in the low-mass region. The HELIOS/3 collaboration has measured dimuon production in 200 GeV/u S-W collisions and 200 GeV p-W collisions at more forward rapidities $y > 3.5$ [7]. The observed $\mu^+\mu^-$ spectrum shows a similar onset of the excess around $m_{\mu\mu} \approx 2m_\pi$. However, the magnitude of the enhancement factor – which we have derived from their data as the integral of the S-W data over the integral of the p-W data in the comparable mass range – is significantly smaller ($\simeq 1.6$). This difference could be explained by a non-linear dependence of the underlying production mechanism. Indeed, the average charged-particle densities accessible by the two experiments, and hence the energy densities, differ by at least a factor of 2 (due to the more central rapidity coverage of the CERES experiment). This, taken together with the onset of the excess at $m_{ee} \simeq 2m_\pi$ and the persistence of the enhancement in the ρ-region, suggests that we observe two-pion annihilation $\pi\pi \rightarrow e^+e^-$.

The CERES collaboration acknowledges the good performance of the CERN PS and SPS accelerators. We are grateful for support by the German Bundesministerium für Forschung und Technologie under grant BMFT 06HD525I, the U.S. Departement of Energy under Contract No. DE-AC02-76CH00016, the MINERVA Foundation, Munich/Germany, the H. Gutwirth Fund and the Israeli Science Foundation.

References

[*] Doctoral thesis of Th. Ullrich and part of doctoral thesis of R. Baur, Universität Heidelberg (1994).
[1] E. V. Shuryak, Phys. Lett. **78B** 150 (1978).
[2] K. Kajantie *et al.*, Phys. Rev. **D34** 2746 (1986).
[3] P. V. Ruuskanen, Nucl. Phys. **A544** 169c (1992).
[4] J. Cleymans, V. V. Goloviznin and K. Redlich, Zeit. Phys. **C59** 495 (1993).
[5] P. Koch, Zeit. Phys. **C57** 283 (1993).
[6] M. C. Abreu *et al.*, Nucl. Phys. **A566** 77c (1994).
[7] M. Masera, in *Proc. of the Eleventh Int. Conf. on Ultra-Relativistic Nucleus-Nucleus Collisions*, Monterey 1995, (to be published).
[8] R. Baur *et al.*, Nucl. Inst. Meth. **A343** 231 (1994).
[9] W. Chen *et al.*, IEEE Trans. Nucl. Sci. **39** 619 (1992).
[10] T. F. Günzel *et al.*, Nucl. Inst. Meth. **A316** 259 (1992).
[11] J. Gläß *et al.*, IEEE Trans. Nucl. Sci. **37** 241 (1990).
[12] T. Åkesson *et al.*, Zeit. Phys. **C** (to be published) (1995).
[13] M. Bourquin and J. M. Gaillard, Nucl. Phys. **B114** 334 (1976).
[14] T. Åkesson *et al.*, Zeit. Phys. **C46** 361 (1992).
[15] T. Alber *et al.*, Nucl. Phys. **A566** 35c (1994).
[16] R. Santo *et al.*, Nucl. Phys. **A566** 61c (1994).
[17] R. Albrecht *et al.*, Zeit. Phys. **C55** 539 (1992).
[18] M. Aguilar-Benitez *et al.*, Zeit. Phys. **C50** 405 (1991).
[19] L. G. Landsberg, Phys. Rev. **128** 301 (1985).
[20] G. J Gounaris and J. J. Sakurai, Phys. Rev. Lett. **21** 244 (1966).
[21] C. P. de los Heros, Weizmann Institute of Science, Ph.D. thesis (to be published).